Supporting Information

Carbene-derived *a*-acyl iminium cations: organic molecules with readily tunable multiple redox processes

*Cassie L. Deardorff, R. Eric Sikma, Christopher P. Rhodes, and Todd W. Hudnall**

Department of Chemistry and Biochemistry, Texas State University, San Marcos, Texas 78666
E-mail: hudnall@txstate.edu

Table of Contents

GENERAL CONSIDERATIONS:

Unless otherwise noted, these procedures were all carried out using typical Schlenk techniques under an atmosphere of nitrogen or in a nitrogen-filled glove box. Solvents were dried and degassed by an Innovative Technology solvent purification system and stored over a 3 Å molecular sieves in a nitrogen-filled glove box. Chloroform-D ($CDCl_3$) was dried over a 3 Å molecular sieves and distilled prior to use. Carbenes **1a**, **1b**, **1c** and **CAAC-Et$_2$** were prepared according to literature procedures.[1–2] All reagents were used as received. NMR spectra were recorded on Bruker Avance 400 MHz/52mm spectrometer. Chemical shifts (δ) are given in ppm and are referenced to the residual solvent: ^{1}H: $CDCl_3$, 7.26 ppm; ^{13}C: 77.0 ppm. Elemental analyses were performed at Midwest Microlabs, LLC (Indianapolis, IN). Melting point determinations were performed on Mel-Temp apparatus and are uncorrected.

SYNTHESIS OF COMPOUNDS:

Synthesis of 2a:

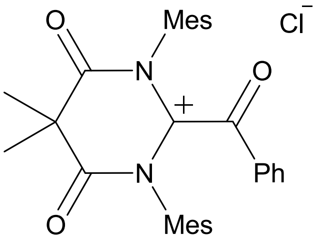

In a nitrogen-filled glovebox, a 100 mL Schlenk flask was charged with **1a** (500 mg, 0.97 mmol) and a magnetic stirring bar. To this flask was added 10 mL of hexanes. Benzoyl Chloride (0.154 mL, 1.33 mmol) was added to the carbene suspension in hexanes. The reaction mixture was allowed to stir at room temperature for 2 hours. During the course of the reaction a light yellow precipitate formed. After 2 hours an additional 30 mL of hexanes was added and allowed to stir for 20 minutes. The solution was removed by cannula, and the remaining volatiles were removed *in vacuo* to afford the desired cation as a light yellow/white solid (602.5 mg, 87.7%). mp 183.6-185.2°C (dec) ^{1}H NMR ($CDCl_3$, 400.13 MHz): δ 1.95 (s, 3H, Mes-CH_3), 2.15 (s, 6H, C(CH_3)$_2$), 2.40 (s, 3H, Mes-CH_3), 2.41 (s, 6H, Mes-CH_3), 2.73 (s, 6H, Mes-CH_3), 6.65 (s, 2H, Mes-CH), 6.83 (s, 2H, Mes-CH), 7.47 (t, ^{3}J = 7.9 Hz, 2H, Ph-CH), 7.61 (t, ^{3}J = 7.5 Hz, 1H, Ph-CH), 8.19 (d, ^{3}J = 7.40 Hz, 2H, Ph-CH). ^{13}C NMR ($CDCl_3$, 100.61 MHz): δ 19.78, 20.37, 20.77, 23.55, 28.96, 55.47, 128.89, 129.73, 129.84, 130.47, 131.07, 135.39, 137.10, 140.33, 141.45, 165.07, 168.77, 179.30. Anal. Calcd. (%) for $C_{31}H_{33}N_2O_3Cl_1$: C: 72.01, H: 6.43, N: 5.42; found: C: 71.56, H: 6.46, N: 5.48.

Synthesis of 2b:

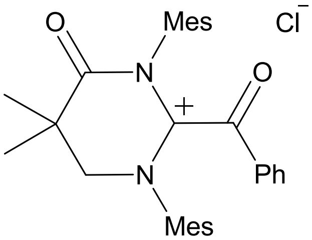

In a nitrogen-filled glovebox, a 100 mL Schlenk flask was charged with **1b** (500 mg, 0.99 mmol) and a magnetic stirring bar. To this flask was added 10 mL of hexanes. Benzoyl Chloride (0.160 mL, 1.38 mmol) was added to the carbene suspension in hexanes. The reaction mixture was allowed to stir at room temperature for 2 hours. During the course of the reaction a light precipitate formed. After 2 hours an additional 30 mL of hexanes was added and allowed to stir for 20 minutes. The solution was removed by cannula and the remaining volatiles were removed *in vacuo* to afford the desired cation as a white solid which was recrystallized from hexanes/DCM (608.1 mg, 87.6%). mp 247.9-250.1°C (dec) ^{1}H NMR ($CDCl_3$, 400.13 MHz): δ 1.81 (s, 3H, C(CH_3)), 1.98 (s, 3H, C(CH_3)), 2.12 (s, 3H, Mes-CH_3), 2.14 (s, 3H, Mes-CH_3), 2.33 (s, 3H, Mes-CH_3), 2.49 (s, 3H, Mes-CH_3), 2.56 (s, 3H, Carbene-CH_3), 2.70 (s, 3H, Carbene-CH_3), 3.92 (d, ^{2}J = 15.0 Hz, 1H, CH_2), 6.61 (s, 1H, Mes-CH), 6.63 (d, ^{2}J = 15.0 Hz, 1H, CH_2), 6.67 (s, 1H, Mes-CH), 6.80 (s, 1H, Mes-CH), 6.87 (s, 1H, Mes-CH), 7.45 (t, ^{3}J = 7.5 Hz, 2H, Ph-CH), 7.59 (t, ^{3}J = 6.5, 1H, Ph-CH), 7.92 (d, ^{3}J = 8.5Hz, 2H, Ph-CH) ^{13}C NMR ($CDCl_3$, 100.61 MHz): δ 0.96, 19.05, 19.45, 19.77, 20.00, 20.71, 20.76, 23.78, 26.34, 38.73, 61.86, 128.86, 129.47, 131.06, 133.53, 134.47, 135.19, 136.17, 136.78, 138.31, 141.01, 162.42, 169.48, 179.45. Despite drying under vacuum for several days, residual dichloromethane could not be removed for elemental analysis: Anal. Calcd. (%) for $C_{31.2}H_{35.4}N_2O_2Cl_{1.4}$ (**2b**-$(CH_2Cl_2)_{0.2}$): C: 72.06, H: 6.86, N: 5.39; found: C: 72.29, H: 6.95, N: 5.34.

Synthesis of 2c:

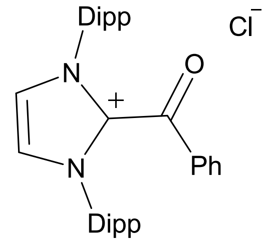

In a nitrogen-filled glovebox, a 100 mL Schlenk flask was charged with **1c** (500 mg, 0.94 mmol) and a magnetic stirring bar. To this flask was added 10 mL of hexanes. Benzoyl Chloride (0.150 mL, 1.29 mmol) was added to the carbene solution in hexanes. The reaction mixture was allowed to stir at room temperature for 12 hours. During the course of the reaction a light yellow precipitate formed. After 12 hours an additional 30 mL of hexanes was added and allowed to stir for 20 minutes. The solution was removed by cannula and the remaining volatiles were removed *in vacuo* to afford the desired cation as a light yellow solid which was recrystallized from hexanes/DCM (680.9 mg, 84.3%). mp 203.9-206.1°C (dec) ^{1}H NMR ($CDCl_3$, 400.13 MHz): δ 1.11 (d, ^3J = 6.8 Hz, 12H, Dipp-C*H*$_3$), 1.20 (d, ^3J = 6.8 Hz, 12H, Dipp-C*H*$_3$), 2.44 (sept, ^3J = 6.8 Hz, 4H, Dipp-C*H*), 7.12 (d, ^3J = 7.8Hz, 4H, Dipp-C*H*), 7.27 (t, ^3J = 7.9Hz, 2H, Dipp-C*H*), 7.37 (m, 4H, Ph-C*H*), 7.51 (t, ^3J = 7.5Hz, 1H, Ph-C*H*), 8.80 (s, 2H, carbene- (C*H*)$_2$). ^{13}C NMR ($CDCl_3$, 100.61 MHz): δ 22.26, 26.18, 29.39, 124.73, 128.10, 132.16, 133.27, 136.24, 140.63, 144.97, 179.05. Despite drying under vacuum for several days, residual dichloromethane could not be removed for elemental analysis: Anal. Calcd. (%) for $C_{35}H_{43}N_2O_1Cl_3$ (**2c**-CH_2Cl_2): C: 68.46, H: 7.06, N: 4.56; found: C: 69.09, H: 7.24, N: 4.56.

Synthesis of 2d:

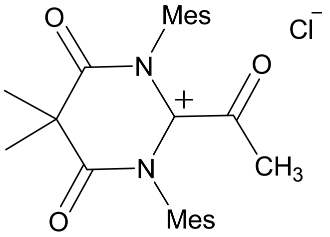

In a nitrogen-filled glovebox, a 100 mL Schlenk flask was charged with **1a** (336 mg, 0.74 mmol) and a magnetic stirring bar. To this flask was added 6 mL of hexanes. Acetyl Chloride (0.094 mL, 1.32 mmol) was added to the carbene solution in hexanes. The reaction mixture was allowed to stir at room temperature for 2 hours. During the course of the reaction a yellow precipitate formed. After 2 hours an additional 30 mL of hexanes was added and allowed to stir for 20 minutes. The solution was removed by cannula, and the remaining volatiles were removed *in vacuo* to afford the desired cation as a yellow solid (154 mg, 45.9%). mp 146.0-148.2°C (dec) ^{1}H NMR ($CDCl_3$, 400.13 MHz): δ 1.05 (s, 3H, Carbene-CH_3), 1.07 (s, 3H, Carbene-CH_3), 1.98 (s, 6H; 3H, Mes-CH_3; Carbonyl-CH_3), 2.18 (s, 3H, Mes-CH_3), 2.32 (s, 3H, Mes-CH_3), 2.37 (s, 6H, Mes-CH_3), 6.72 (s, 2H, Mes-CH), 7.00 (s, 2H, Mes-CH). ^{13}C NMR ($CDCl_3$, 100.61 MHz): δ 1.19, 21.20, 27.08, 53.53, 56.20, 128.43, 129.36, 142.60, 162.98, 168.34, 186.25. Anal. Calcd. (%) for $C_{26}H_{31}N_2O_3Cl$ (**2d**): C: 68.46, H: 7.06, N: 4.56; found: C: 69.09, H: 7.24, N: 4.56.

Synthesis of 4:

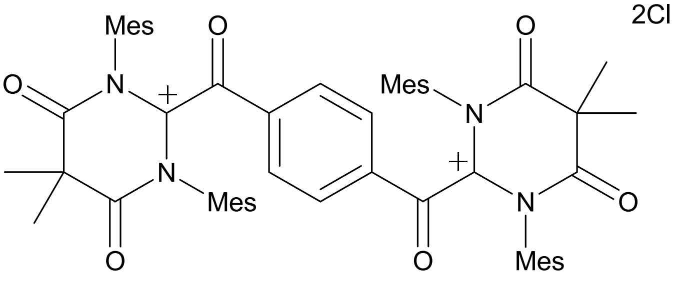

In a nitrogen-filled glovebox, a 100 mL Schlenk flask was charged with **1a** (100 mg, 0.27 mmol) and a magnetic stirring bar. To this flask was added 5 mL of dichloromethane. Terephthaloyl Chloride (27.0 mg, 0.133 mmol) was added to the DAC solution in dichlormethane. The reaction mixture was allowed to stir at room temperature for 2 hours. After 2 hours an additional 20 mL of hexanes was added and allowed to stir for 10 minutes. The solution was removed by cannula and the remaining volatiles were removed in vacuo to afford the desired cation as a white solid (167.5 mg, 26.4%). mp 222.0-224.0°C (dec) ^{1}H NMR ($CDCl_3$, 400.13 MHz): δ

1.92 (s, 6H, C(CH_3)$_2$), 2.22 (s, 12H, Mes-CH$_3$), 2.34 (s, 6H, C(CH_3)$_2$), 2.41 (s, 12H, Mes-CH_3), 2.51 (s, 12H, Mes-CH_3), 6.65 (s, 4H, Mes-CH), 6.89 (s, 4H, Mes-CH), 8.35 (bs, 4H, C$_6H_4$). ^{13}C NMR (CDCl$_3$, 100.61 MHz): δ 19.75, 20.91, 23.53, 28.77, 55.53, 128.42, 130.25. 130.86, 135.04, 135.81, 139.99, 142.02, 164.19, 168.32, 178.41. Despite drying under vacuum for several days, residual dichloromethane could not be removed for elemental analysis: Anal. Calcd. (%) for $C_{56.5}H_{61}N_4O_6Cl_3$ (**4**-(CH$_2$Cl$_2$)$_{0.5}$): C: 67.96, H: 6.16, N: 5.61; found: C: 68.38, H: 6.19, N: 5.54.

Synthesis of CAAC-Et$_2$-COPh (S1):

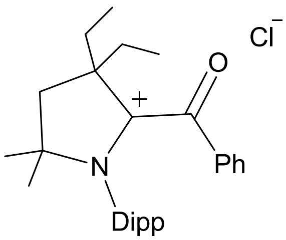

In a nitrogen-filled glovebox, a 50 mL Schlenk flask was charged with **CAAC-Et$_2$** (100 mg, 0.32 mmol) and a magnetic stirring bar. To this flask was added 5 mL of hexanes. Benzoyl Chloride (0.0371 mL, 0.32 mmol) was added to the carbene solution. The reaction mixture was allowed to stir at room temperature for 2 hours. During the course of the reaction a white fluffy precipitate was formed. After 2 hours an additional 30 mL of hexanes was added and allowed to stir for 20 minutes. The solution was removed by cannula and the remaining volatiles were removed *in vacuo* to afford the desired cation as an off-white solid (63.2 mg, 43.6%). This compound was only characterized by ^{1}H NMR and used without further purification. ^{1}H NMR (CDCl$_3$, 400.13 MHz): δ 0.82 (d, ^3J = 6.0 Hz, 6H, Dipp-CH_3), 0.90 (t, ^3J = 7.4 Hz, 6H, Et-CH_3), 1.36 (d, ^3J = 6.3 Hz, 6H, Dipp-CH_3), 1.76 (s, 6H, C(CH_3)$_2$) 2.22 (m, 2H, Et-CH_2), 2.50 (m, 2H, Et-CH_2), 3.02 (s, 2H, Carbene-CH_2), 3.19 (sept. (br), ^3J = 6.4 Hz, 2H, Dipp-CH), 7.22 (d, ^3J = 7.8 Hz, 2H, Dipp-CH), 7.41 (t, ^3J = 7.7 Hz, 1H, Dipp-CH), 7.67 (m, 3H, Ph-CH), 8.60 (d, ^3J = 6.7 Hz, 2H, Ph-CH).

Synthesis of 3a:

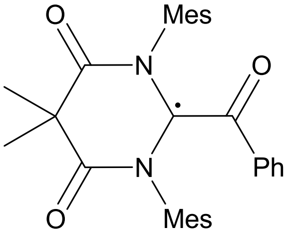

In a nitrogen-filled glovebox, a 50 mL Schlenk flask was charged with **2a** (100 mg, 0.21 mmol) and a magnetic stirring bar. To this flask was added 10 mL of benzene. TDAE (22.5 µL, 0.10 mmol) was added to the solution which resulted in the immediate formation of a dark red suspension. This suspension was allowed to stir at room temperature for 2 hours, after which time the reaction mixture was filtered over Celite. The solution was transferred into a clean 50 mL Schlenk flask and all volatiles were removed *in vacuo* to afford the desired radical as a deep red solid. (42.6 mg, 45.5%)

Synthesis of 3b:

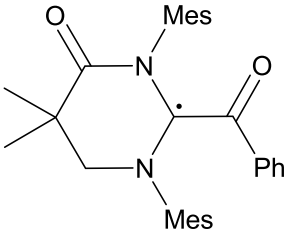

In a nitrogen-filled glovebox, a 50 mL Schlenk flask was charged with **2b** (100 mg, 0.21 mmol) and a magnetic stirring bar. To this flask was added 10 mL of benzene. TDAE (23.1 µL, 0.10 mmol) was added to the solution which resulted in the immediate formation of a dark red suspension. This suspension was allowed to stir at room temperature for 2 hours, after which time the reaction mixture was filtered over Celite. The solution was transferred into a clean 50 mL Schlenk flask and all volatiles were removed *in vacuo* to afford the desired radical as a rust red solid. (63.2 g, 68.0%)

Synthesis of 3c:

In a nitrogen-filled glovebox, a 50 mL Schlenk flask was charged with **2c** (100 mg, 0.20 mmol) and a magnetic stirring bar. To this flask was added 10 mL of benzene. Potassium graphite (25 mg, 0.18 mmol) was added to the solution which resulted in the immediate formation of a dark blue suspension. This suspension was allowed to stir at room temperature for 2 hours, after which time the reaction mixture was filtered over Celite. The solution was transferred into a clean 50 mL Schlenk flask and all volatiles were removed *in vacuo* to afford the desired radical as a dark purple solid. (54.8 mg, 58.7%)

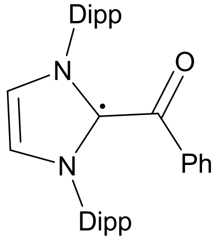

Synthesis of 3d:

In a nitrogen-filled glovebox, a 50 mL Schlenk flask was charged with **2d** (50 mg, 0.12 mmol) and a magnetic stirring bar. To this flask was added 10 mL of benzene. TDAE (14.04 µL, 0.060 mmol) was added to the solution which resulted in the immediate formation of a deep orange suspension. This suspension was allowed to stir at room temperature for 2 hours, after which time the reaction mixture was filtered over Celite. The solution was transferred into a clean 50 mL Schlenk flask and all volatiles were removed *in vacuo* to afford the desired radical as a deep orange solid. (24.7 mg, 49.4%)

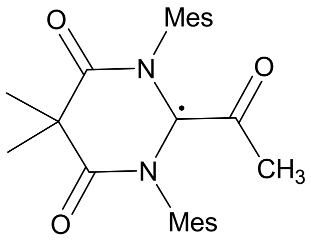

Synthesis of 5:

In a nitrogen-filled glovebox, a 50 mL Schlenk flask was charged with **4** (50 mg, 0.065 mmol) and a magnetic stirring bar. To this flask was added 10 mL of DCM. TDAE (24.3 µL, 0.10 mmol) was added to the solution which resulted in the immediate formation of a dark red-orange solution. This solution was allowed to stir at room temperature for 2 hours after which time all volatiles were removed in vacuo. The resulting solid was extracted with benzene (10 mL) and filtered. Removal of the solvent afforded the desired diradical as a brown/red solid. (10.3 mg, 34.2%) mp 164-168°C.

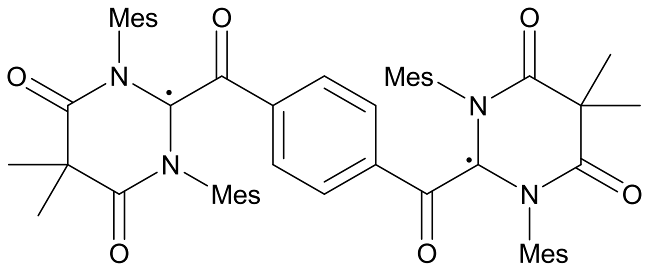

Synthesis of S1-radical:

In a nitrogen-filled glovebox, a 20 mL vial was charged with **S1** (25 mg, 0.06 mmol) and a magnetic stirring bar. To this flask was added 5 mL of benzene. Tetrakis(dimethylamino)ethylene (6.56 µL, 0.03 mmol) was added to the CAAC-COPh Cation solution in benzene. This solution was allowed to stir at room temperature for 2 hours. After 2 hours the reaction mixture was filtered and the solution was put into a clean 50 mL Schlenk flask. The remaining volatiles were removed *in vacuo* to afford the desired radical as a red solid.

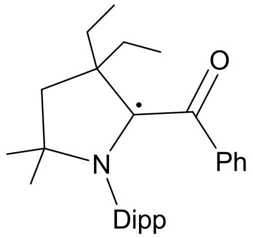

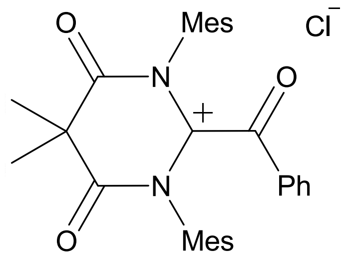

2a

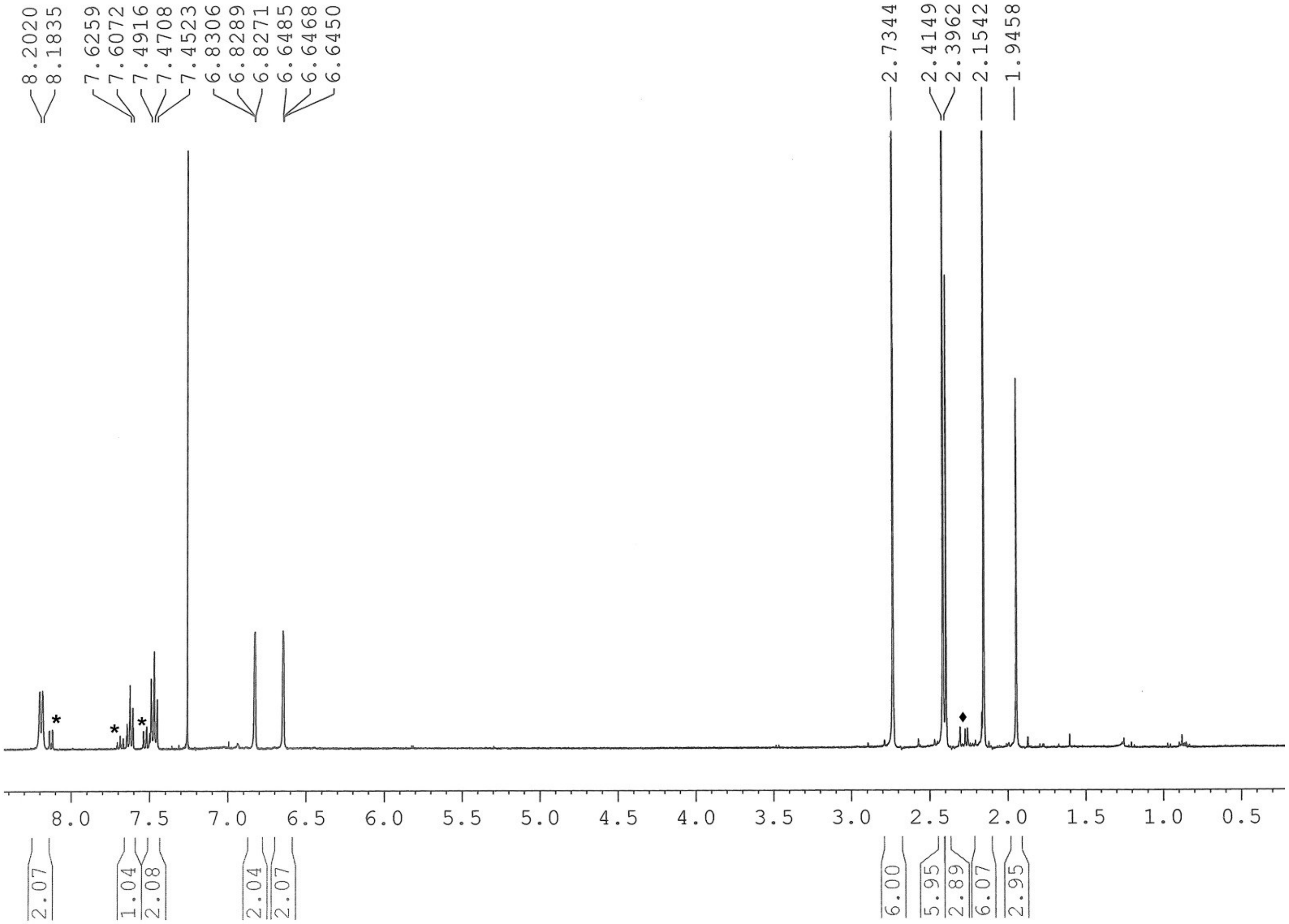

^{1}H NMR spectrum of **2a** in $CDCl_3$ (* denotes residual benzoyl chloride, ♦ denotes small impurity).

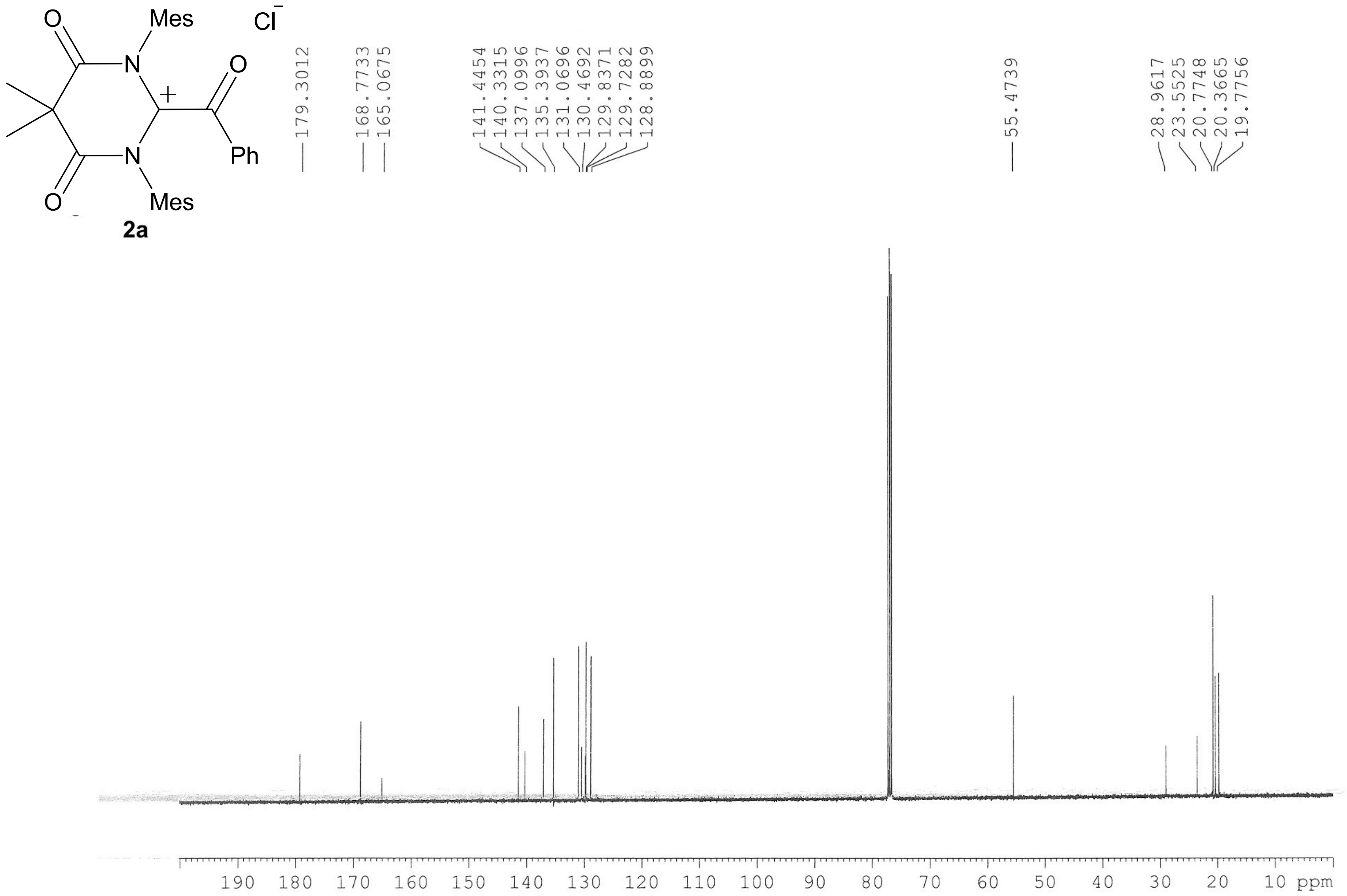

^{13}C NMR spectrum of **2a** in $CDCl_3$.

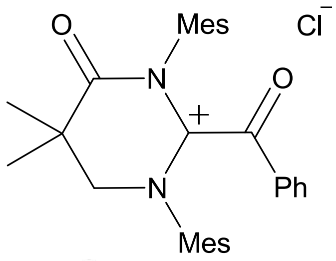

2b

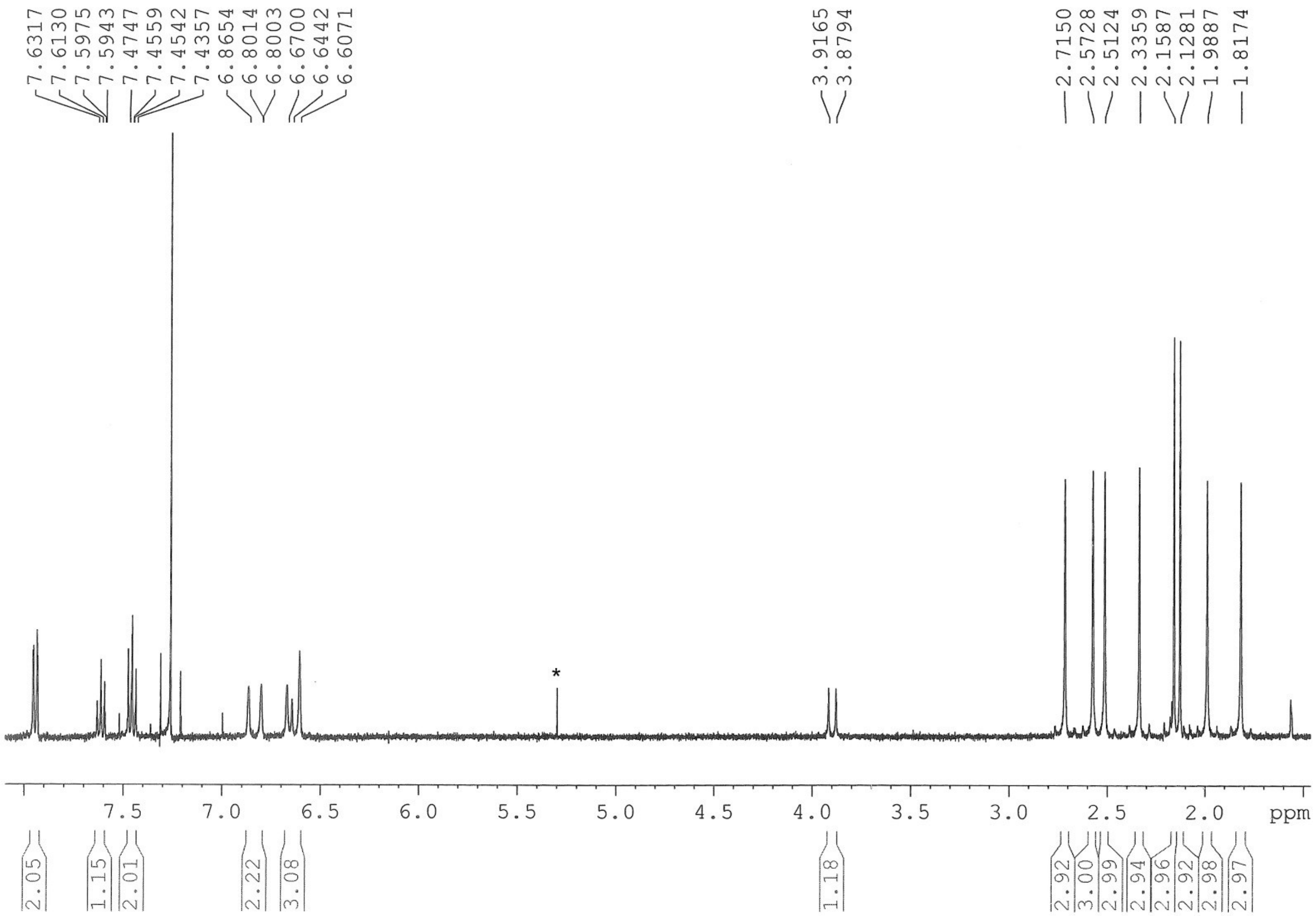

^{1}H NMR spectrum of **2b** in $CDCl_3$ (* denotes residual dichloromethane).

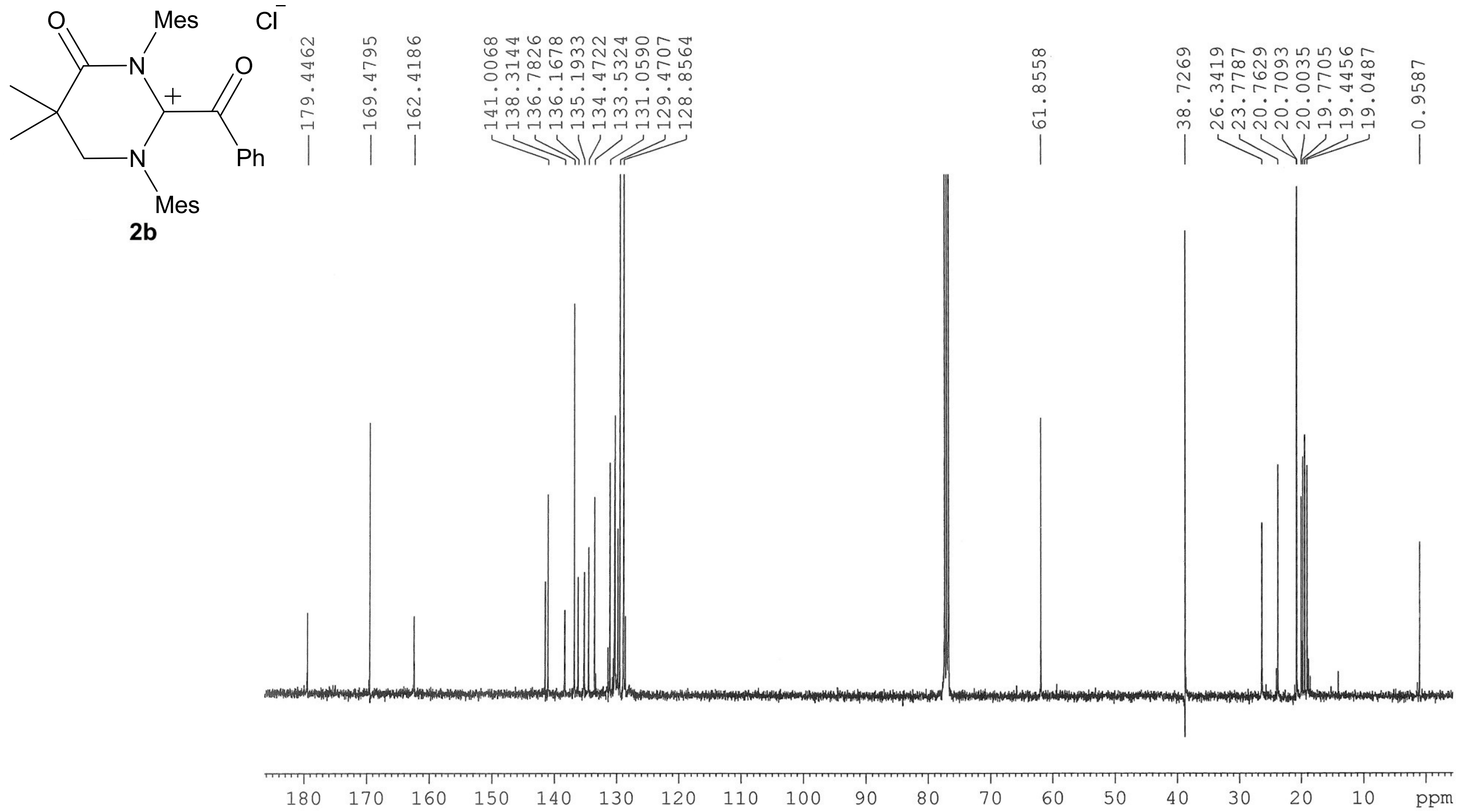

^{13}C NMR spectrum of **2b** in CDCl$_3$.

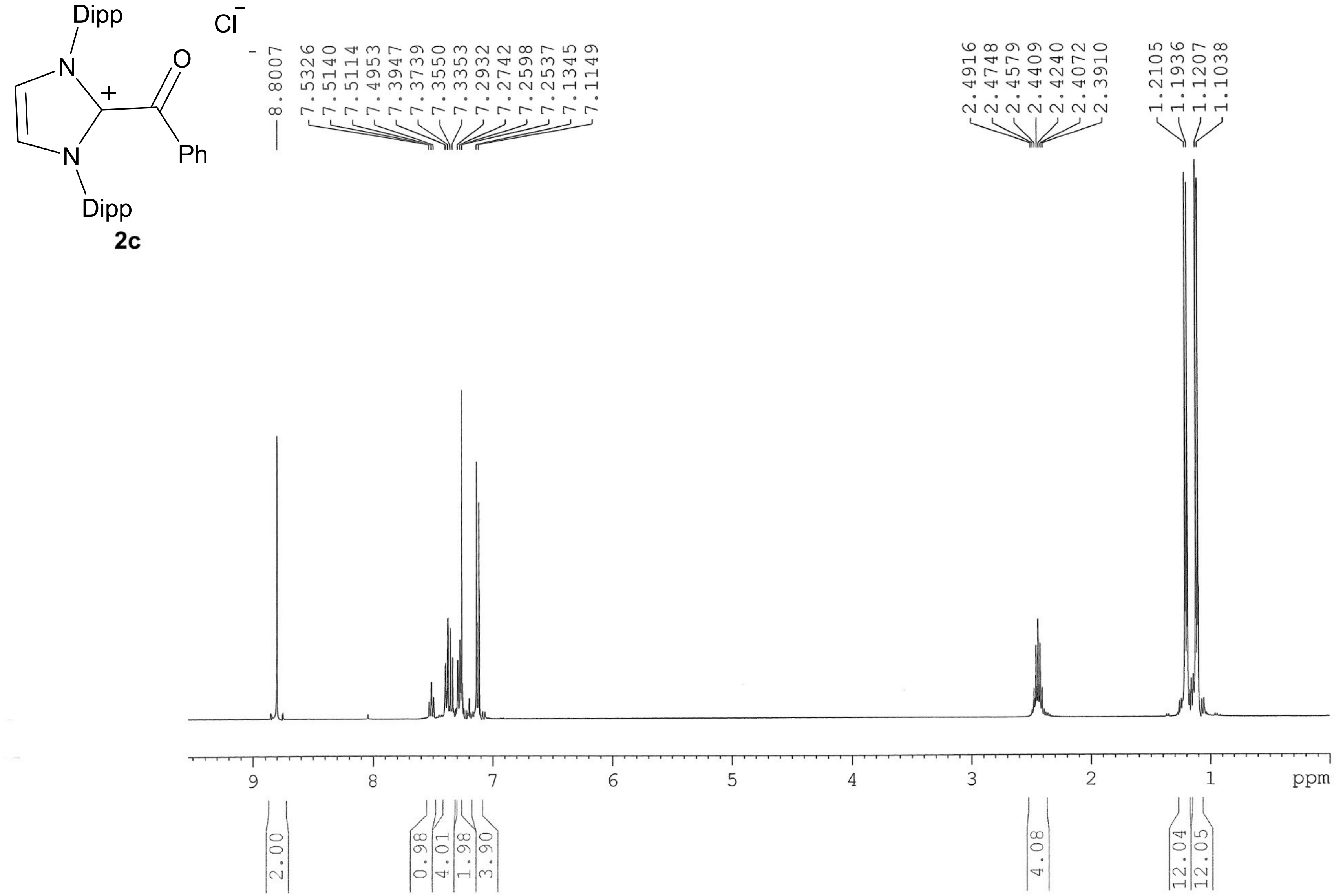

2c

^{1}H NMR spectrum of **2c** in $CDCl_3$.

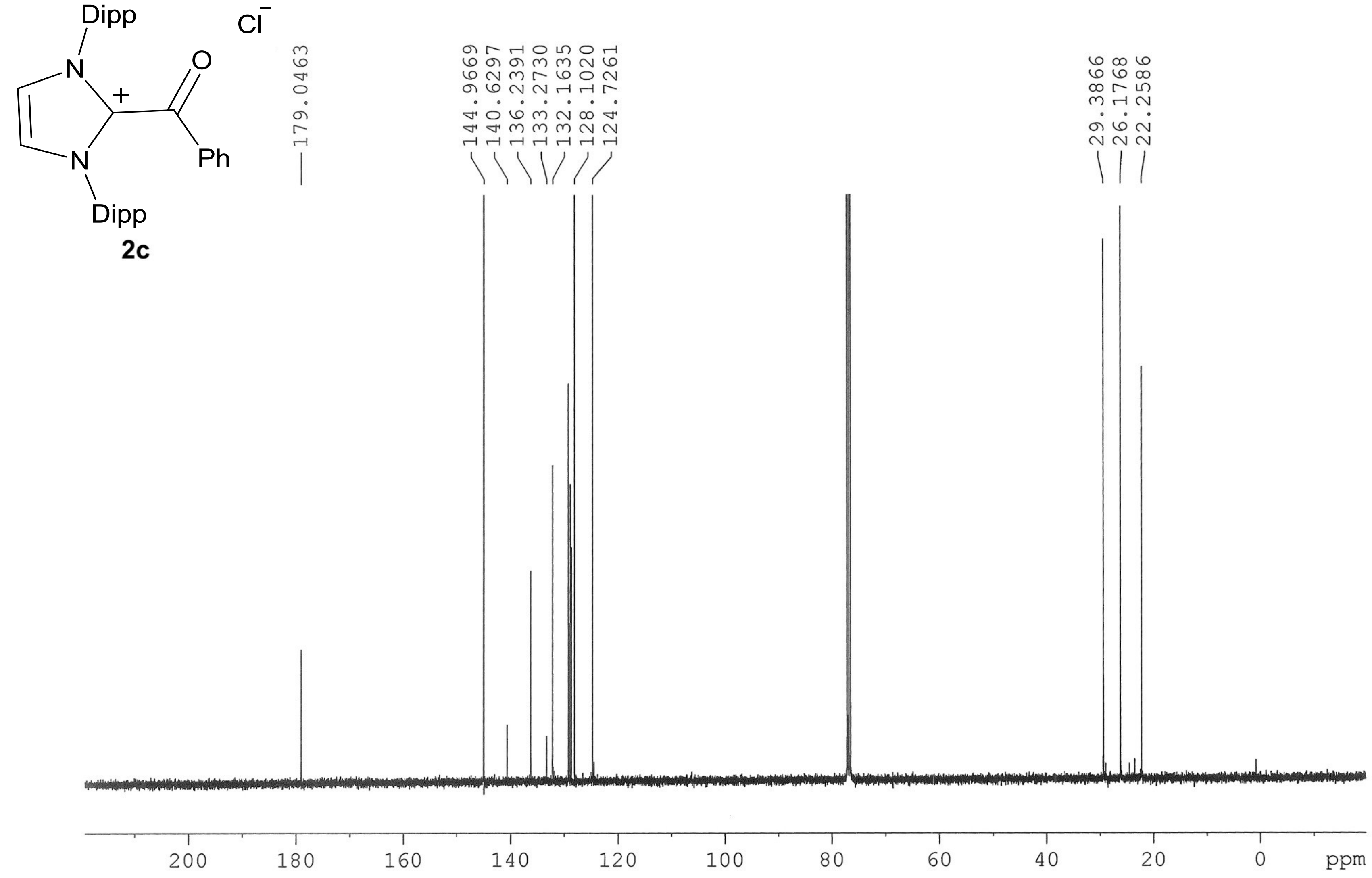

^{13}C NMR spectrum of **2c** in CDCl$_3$.

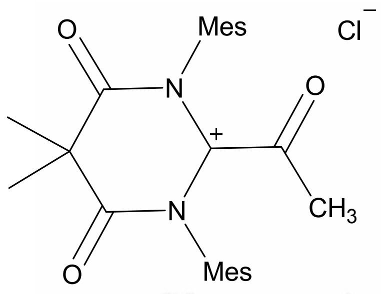

2d

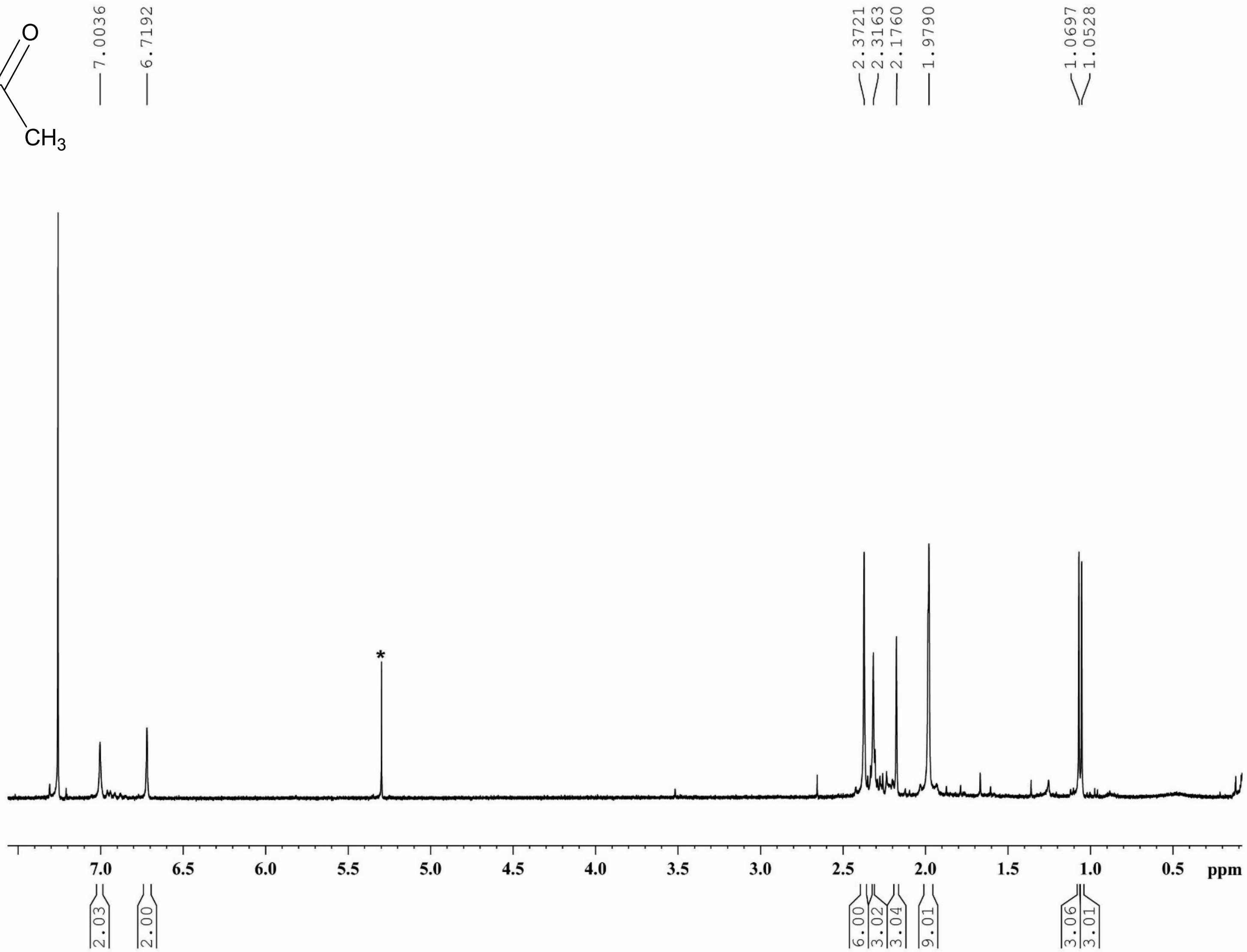

^{1}H NMR spectrum of **2c** in $CDCl_3$. (* denotes residual dichloromethane)

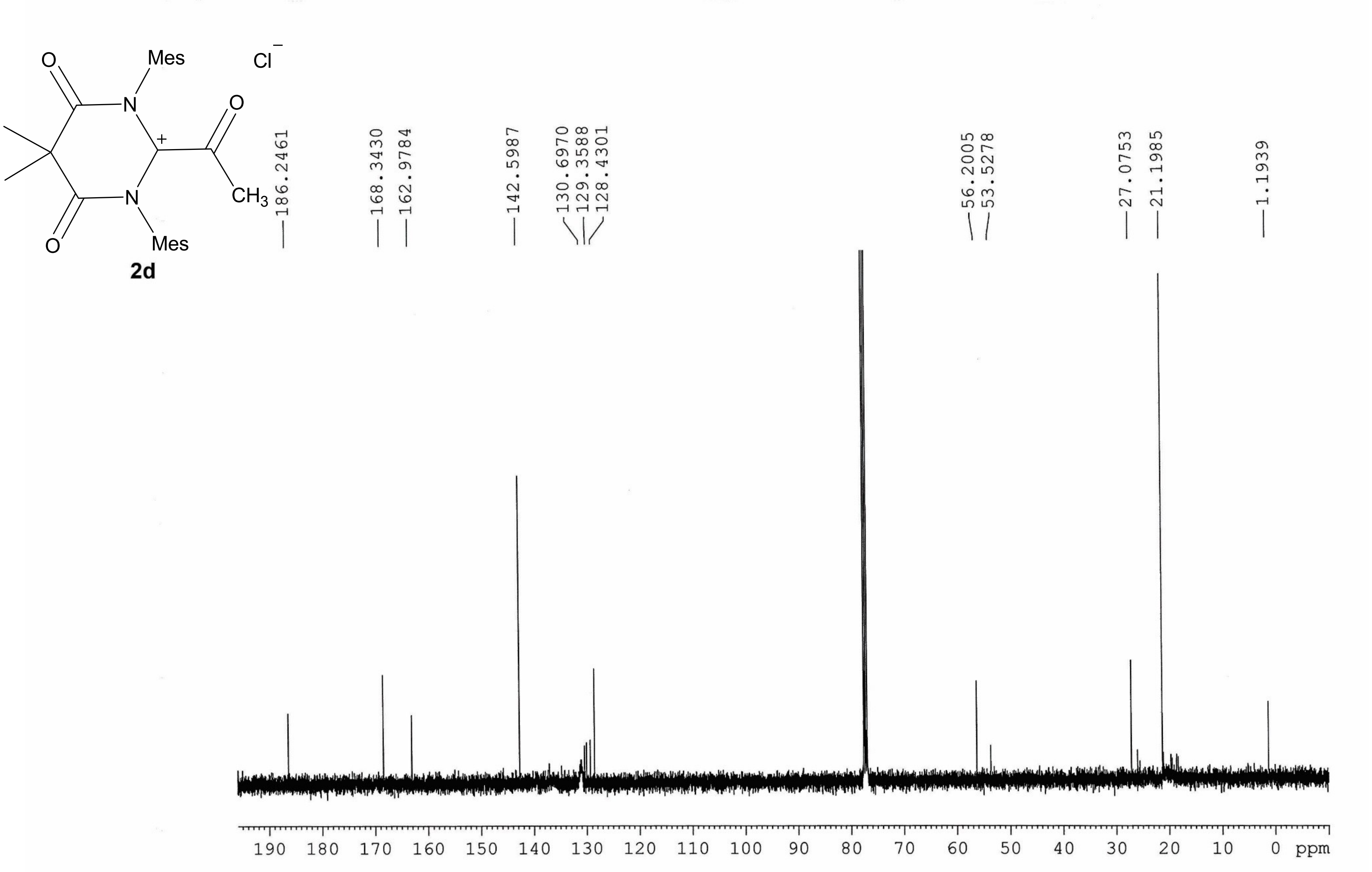

^{13}C NMR spectrum of **2d** in CDCl$_3$

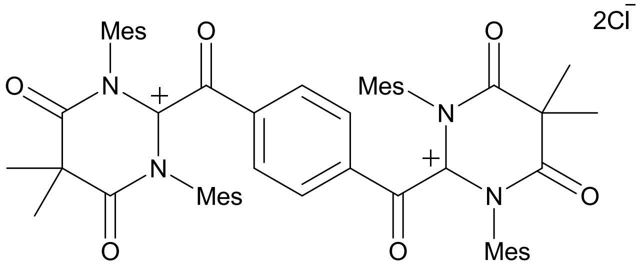

4

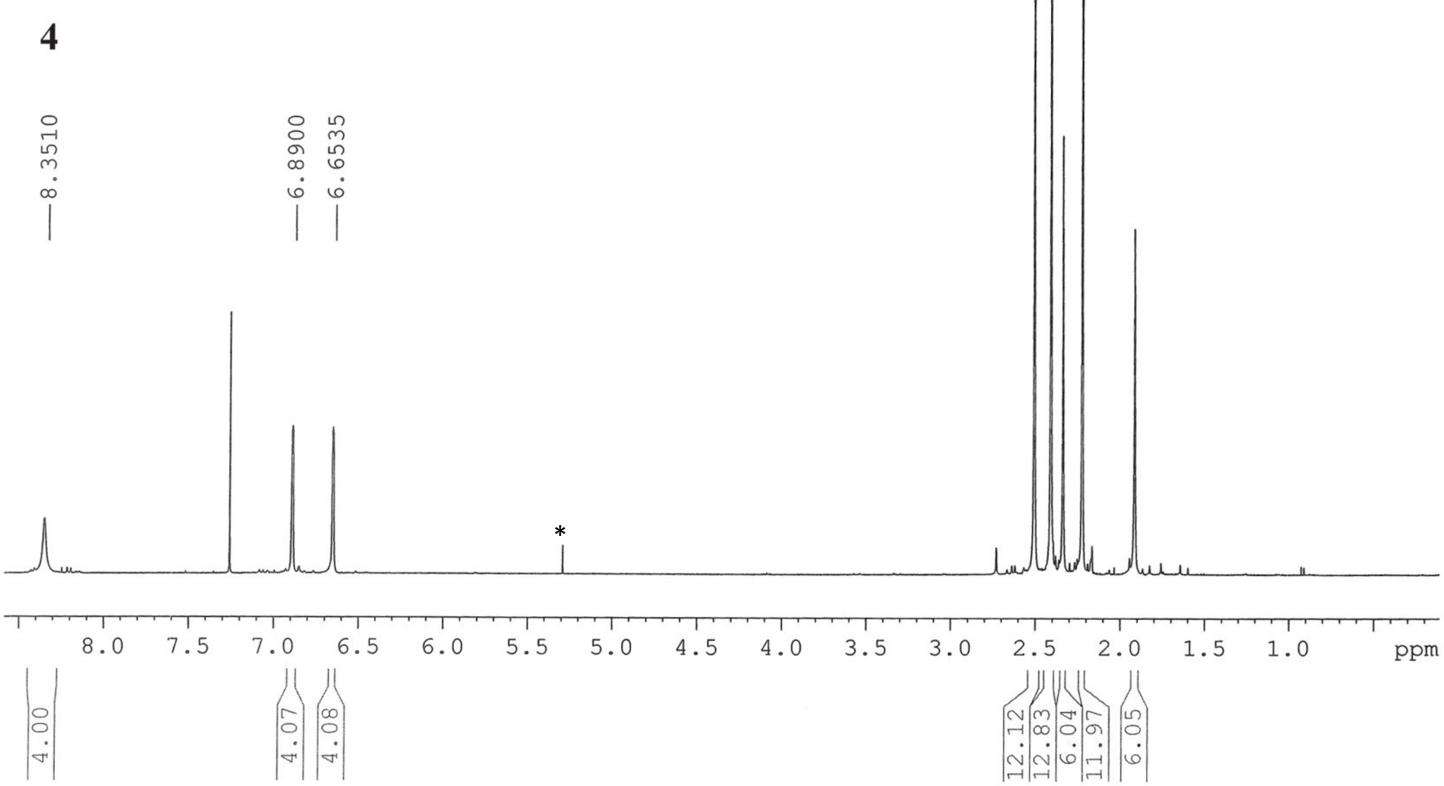

^{1}H NMR spectrum of **4** in $CDCl_3$ (* denotes residual dichloromethane).

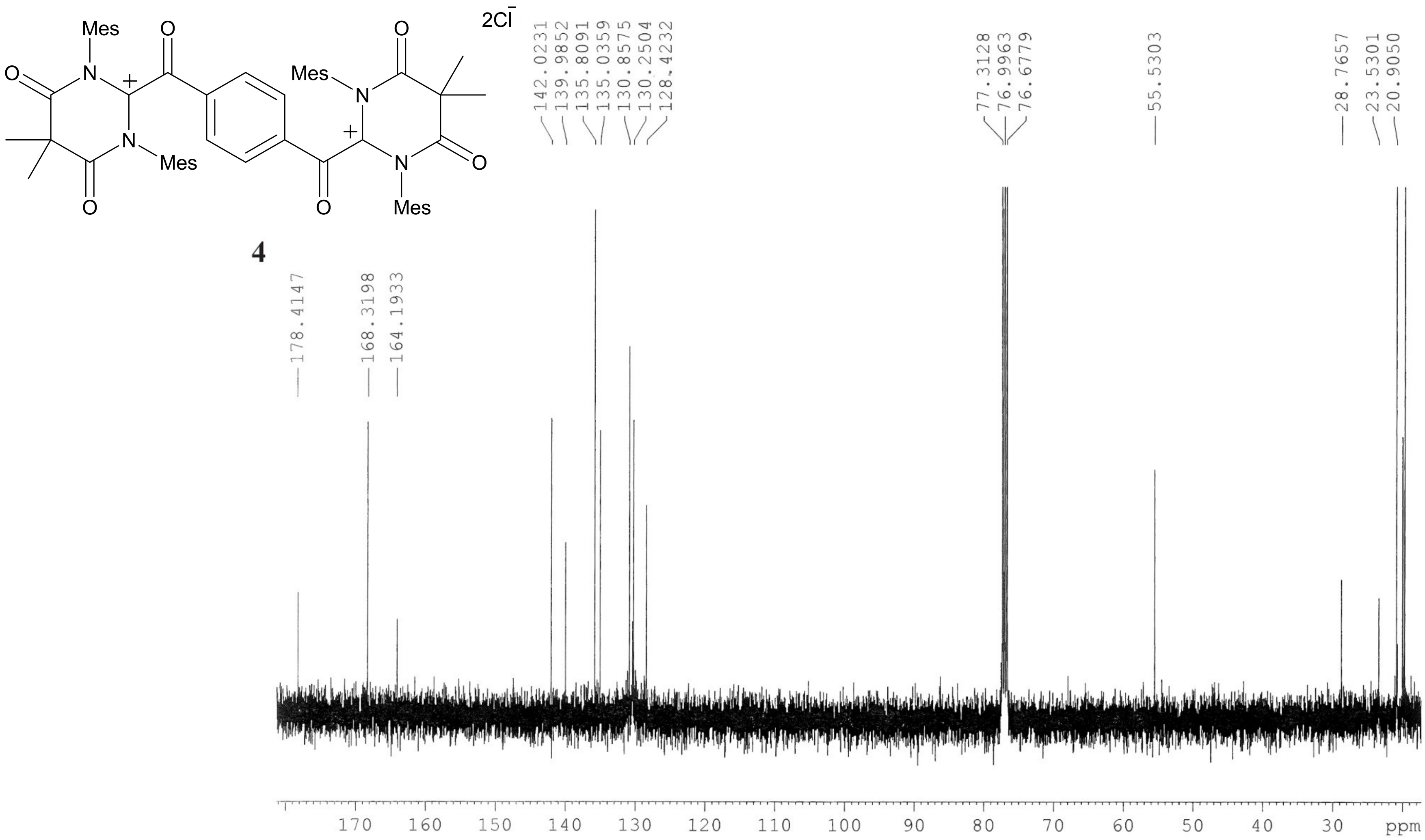

^{13}C NMR spectrum of **4** in $CDCl_3$.

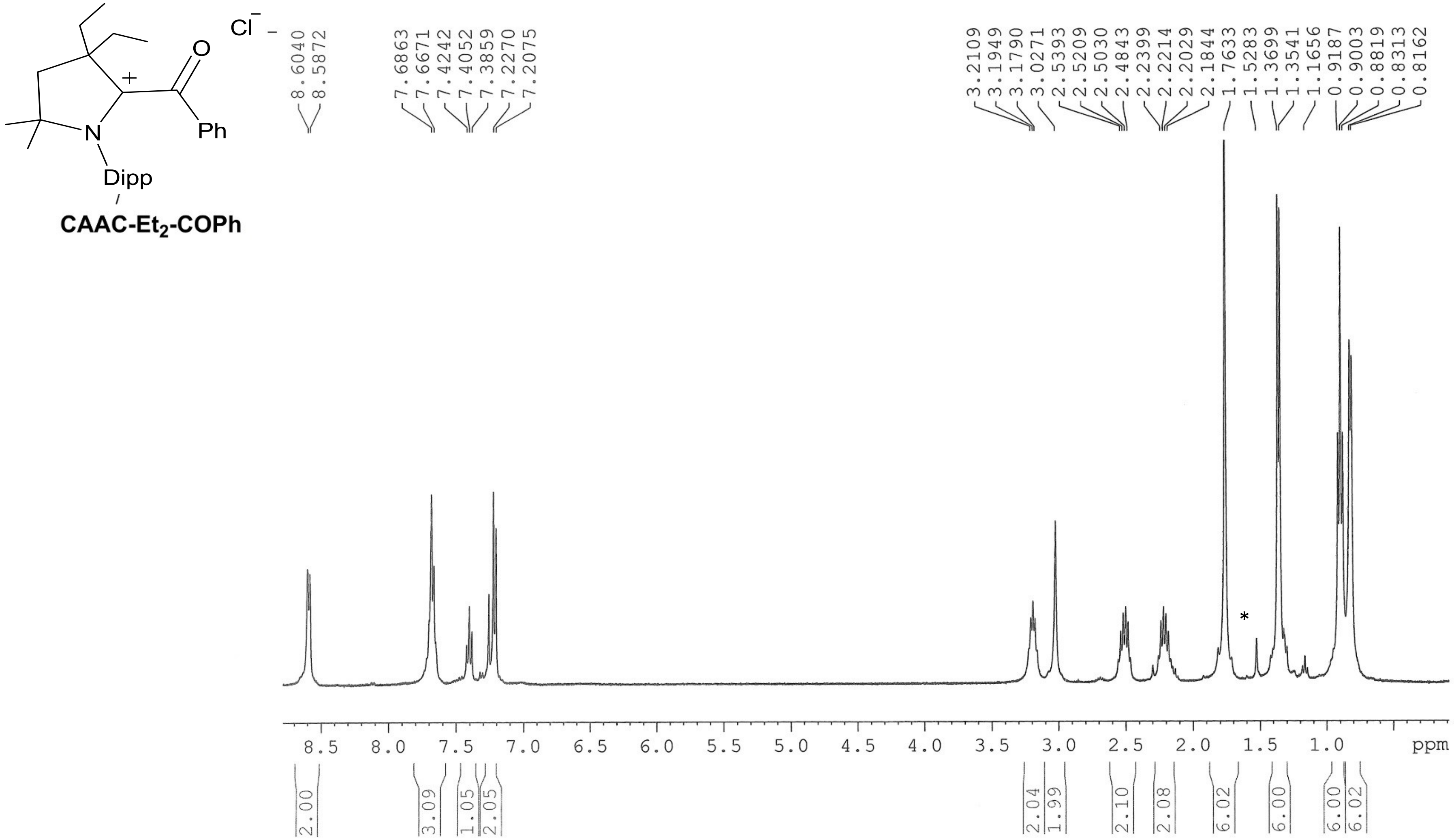

^{1}H NMR spectrum of **CAAC-Et$_2$-COPh** (**S1**) in CDCl$_3$ (*denotes small impurity).

CYCLIC VOLTAMMETRY

General Considerations: Electrochemical experiments were performed with an analyzer from CH Instruments (Model 600D) with a glassy carbon working, platinum wire counter electrodes. The reference electrode was built from a silver wire inserted into a small glass tube fitted with a porous frit and filled with a $AgNO_3$ solution in THF (0.01 M). Ferrocene was used for calibration, and all reduction potentials are reported with respect to the $E_{1/2}$ of the Fc^+/Fc redox couple. All cyclic voltammograms were recorded in dichloromethane using $n Bu_4NPF_6$ as the electrolyte (0.1M) at a scan rate of 100 mVs^{-1}.

Theoretical Specific Capacity and Specific Capacitance Calculations: Theoretical specific capacities (mAh/g) were determined using the compound formula weight and the number of electrons involved in the reaction. Theoretical specific capacitance values were determined by using the compound formula weight, the number of electrons in the reaction, and the experimental voltage range. The experimental voltage range was determined from the onset of the first reduction wave to the conclusion of the second wave. Since compound **2c** was not reversible over the full voltage range, only the first reduction wave was used for this compound for the specific capacitance and specific capacity values. These calculations showed theoretical specific capacitance values ranging from 264.5 F/g to 379.9 F/g and theoretical specific capacities of 51–118 mAh/g.

Discussion of Cyclic Voltammertry: The electrochemical properties of all four cations were then interrogated by cyclic voltammetry (CV) (see Figure 3). Remarkably, modifying the structure of the cation through varying the carbene demonstrated the ability to tune the redox potential as well as reversibility of the redox events. The cyclic voltammetry supports that these ions undergo two sequential 1-electron reduction processes from the fully oxidized cation (**A**), to the neutral radical (**B**), and then to the fully reduced enolate anion (**C**) as described in Scheme S1.

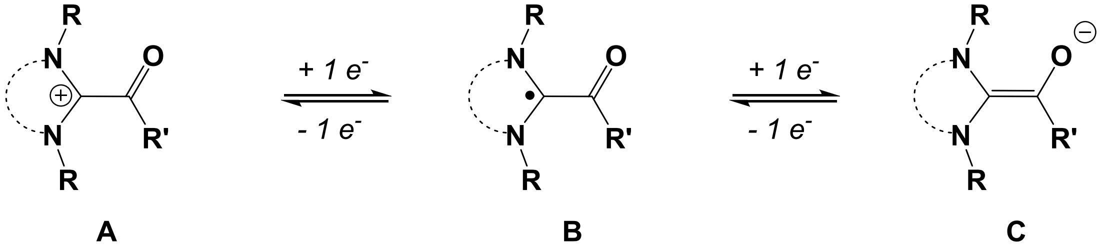

Scheme S1. Sequential reduction of α-iminium caions **A** to neutral radicals **B,** and enolates **C**.

Table S1: Values were recorded from the experimentally obtained cyclic voltammogram and were referenced to ferrocene. Ferrocene was measured to be +0.51 V vs. Ag/AgCl; Li/Li+ is −3.237 vs Ag/AgCl.

			R1		O1		Ratio of peak current (O1/R1)	R2		O2		Ratio of peak current (O2/R2)
Scan Rate	Compound	Cycle number	Peak voltage (V vs Fc)	Peak current (A)	Peak voltage (V vs Fc)	Peak current (A)		Peak voltage (V vs Fc)	Peak current (A)	Peak voltage (V vs Fc)	Peak current (A)	
0.1 V/s	DAC-COPh	1	-0.532	8.95E-06	-0.430	7.54E-06	0.84	-1.114	7.08E-06	-1.015	6.57E-06	0.93
		2	-0.536	7.22E-06	-0.431	8.05E-06	1.12	-1.116	7.34E-06	-1.013	7.24E-06	0.99
		3	-0.540	7.70E-06	-0.430	8.12E-06	1.05	-1.117	8.02E-06	-1.012	7.51E-06	0.94
		4	-0.536	7.51E-06	-0.427	7.36E-06	0.98	-1.113	7.52E-06	-1.011	6.92E-06	0.92
		5	-0.536	6.74E-06	-0.430	6.77E-06	1.00	-1.113	6.80E-06	-1.014	6.27E-06	0.92
0.01V/s	DAC-COPh	1	-0.539	2.80E-06	-0.426	2.30E-06	0.82	-1.108	2.32E-06	-1.014	1.58E-06	0.68
		2	-0.537	2.50E-06	-0.421	2.60E-06	1.04	-1.108	2.46E-06	-1.013	1.74E-06	0.71
		3	-0.537	2.77E-06	-0.420	2.67E-06	0.96	-1.110	2.77E-06	-1.011	1.89E-06	0.68
		4	-0.537	2.78E-06	-0.419	2.67E-06	0.96	-1.108	2.76E-06	-1.010	1.92E-06	0.70
		5	-0.536	2.76E-06	-0.418	2.70E-06	0.98	-1.106	2.76E-06	-1.007	1.92E-06	0.70
0.001V/s	DAC-COPh	1	-0.513	1.25E-06	-0.418	1.48E-06	1.18	-1.077	1.05E-06	-1.011	3.64E-07	0.35
		2	-0.507	1.45E-06	-0.416	1.51E-06	1.04	-1.059	7.74E-07	-1.011	3.14E-07	0.41
		3	-0.506	1.47E-06	-0.419	1.44E-06	0.98	-1.065	1.09E-06	-1.009	3.82E-07	0.35
		4	-0.509	1.52E-06	-0.421	1.42E-06	0.94	-1.062	1.04E-06	-1.013	3.70E-07	0.35
		5	-0.508	1.54E-06	-0.426	1.49E-06	0.97	-1.066	9.51E-07	-1.013	3.19E-07	0.34
0.1 V/s	MAAC-COPh	1	-1.029	1.41E-05	-0.926	8.86E-06	0.63	-1.604	6.44E-06	-1.506	5.18E-06	0.80
		2	-1.029	1.16E-05	-0.929	8.87E-06	0.77	-1.604	6.23E-06	-1.511	5.08E-06	0.82
		3	-1.026	1.14E-05	-0.927	8.65E-06	0.76	-1.604	6.21E-06	-1.509	5.13E-06	0.83
		4	-1.025	1.14E-05	-0.930	8.65E-06	0.76	-1.604	6.29E-06	-1.507	5.14E-06	0.82
		5	-1.027	1.14E-05	-0.928	8.72E-06	0.76	-1.604	6.36E-06	-1.510	5.16E-06	0.81
0.01 V/s	MAAC-COPh	1	-1.018	5.23E-06	-0.935	4.16E-06	0.79	-1.591	2.57E-06	-1.522	9.79E-07	0.38
		2	-1.017	5.30E-06	-0.934	4.20E-06	0.79	-1.591	2.61E-06	-1.521	1.02E-06	0.39
		3	-1.018	5.35E-06	-0.935	4.26E-06	0.80	-1.591	2.79E-06	-1.520	1.04E-06	0.37
		4	-1.018	5.41E-06	-0.936	4.31E-06	0.80	-1.590	2.83E-06	-1.517	1.11E-06	0.39
		5	-1.018	5.48E-06	-0.935	4.37E-06	0.80	-1.591	2.80E-06	-1.521	1.06E-06	0.38
0.1 V/s	iPr-COPh	1	-1.424	1.32E-05	-1.241	9.19E-06	0.70	Not Reversible				
		2	-1.402	9.55E-06	-1.246	8.03E-06	0.84					
		3	-1.394	8.44E-06	-1.246	7.57E-06	0.90					
		4	-1.394	7.92E-06	-1.246	7.33E-06	0.93					
		5	-1.389	7.70E-06	-1.251	7.20E-06	0.94					
0.01 V/s	iPr-COPh	1	-1.376	5.14E-06	-1.262	4.68E-06	0.91					
		2	-1.376	4.15E-06	-1.262	4.58E-06	1.10					
		3	-1.372	5.06E-06	-1.261	4.42E-06	0.87					
		4	-1.371	5.02E-06	-1.262	4.50E-06	0.90					
		5	-1.371	5.03E-06	-1.261	4.52E-06	0.90					
0.1 V/s	DAC-COCH$_3$	1	-0.473	9.78E-06	-0.385	5.53E-06	0.57	-1.068	5.10E-06	-0.960	4.19E-06	0.82
		2	-0.475	5.74E-06	-0.385	5.35E-06	0.93	-1.065	4.81E-06	-0.958	4.08E-06	0.85
		3	-0.473	5.67E-06	-0.384	5.44E-06	0.96	-1.068	4.85E-06	-0.959	4.26E-06	0.88
		4	-0.476	5.90E-06	-0.384	5.52E-06	0.94	-1.069	5.04E-06	-0.959	4.35E-06	0.86
		5	-0.476	5.93E-06	-0.387	5.53E-06	0.93	-1.066	5.04E-06	-0.962	4.31E-06	0.86
0.01 V/s	DAC-COCH$_3$	1	-0.465	3.11E-06	-0.387	3.06E-06	0.98	-1.055	1.65E-06	-0.984	9.39E-07	0.57
		2	-0.465	3.21E-06	-0.387	3.07E-06	0.96	-1.053	1.67E-06	-0.981	1.01E-06	0.61
		3	-0.464	3.21E-06	-0.386	3.06E-06	0.96	-1.052	1.53E-06	-0.982	1.02E-06	0.67
		4	-0.465	3.20E-06	-0.388	3.09E-06	0.97	-1.054	1.62E-06	-0.980	9.22E-07	0.57
		5	-0.463	3.22E-06	-0.387	3.02E-06	0.94	-1.052	1.64E-06	-0.980	8.36E-07	0.51

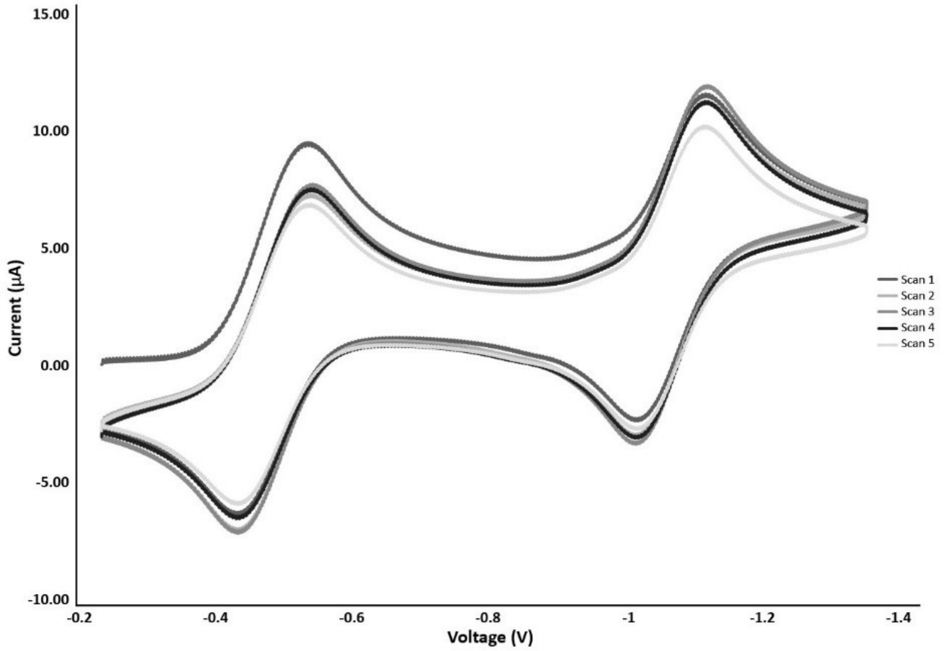

Figure S1: Cyclic voltammogram of imminum cation **2a** recorded in dichloromethane ($n\mathrm{Bu}_4\mathrm{NPF}_6$ 0.1M, 100mVs^{-1} vs. Fc/Fc^{+}).

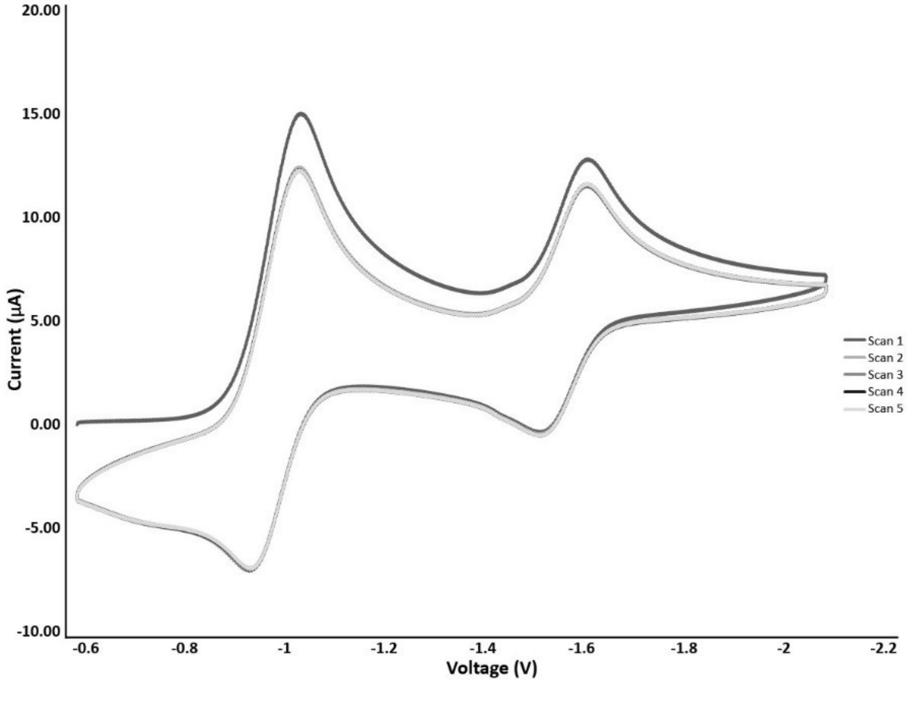

Figure S2: Cyclic voltammogram of imminum cation **2b** recorded in dichloromethane over 5 scans ($n\mathrm{Bu}_4\mathrm{NPF}_6$ 0.1M, 100mVs^{-1} vs. Fc/Fc^{+}).

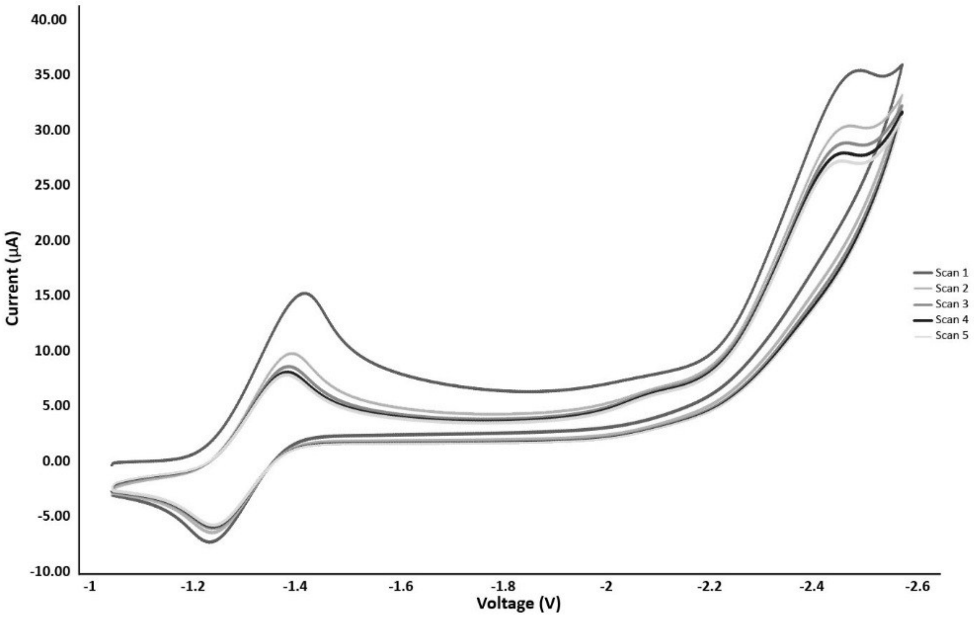

Figure S3: Cyclic voltammogram of imminum cation **2c** recorded in dichloromethane over 5 scnas (*n*Bu_4NPF_6 0.1M, 100mVs^{-1} vs. Fc/Fc^+).

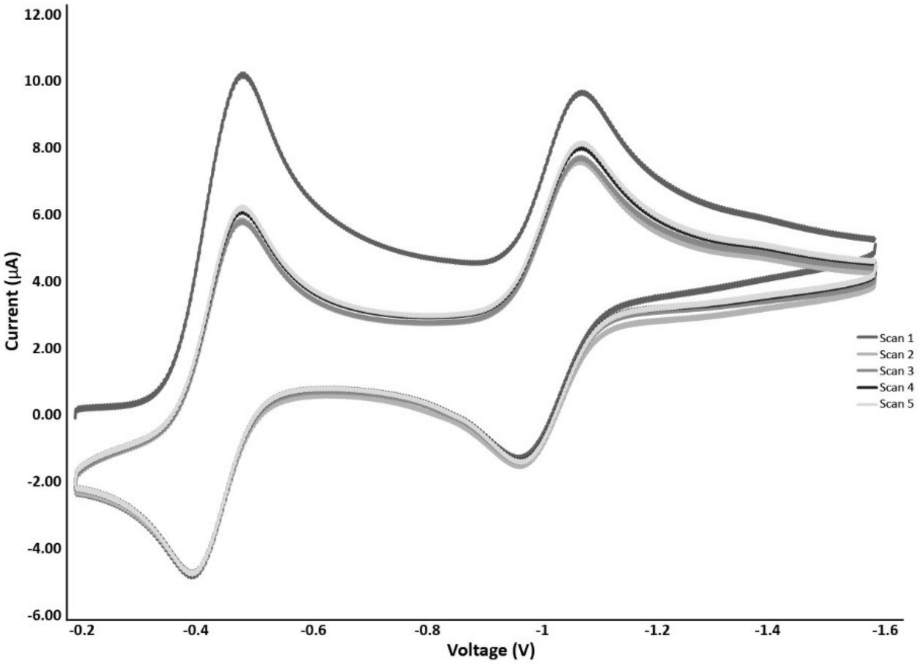

Figure S4: Cyclic voltammogram of imminum cation **2d** recorded in dichloromethane over five scans (*n*Bu_4NPF_6 0.1M, 100mVs^{-1} vs. Fc/Fc^+).

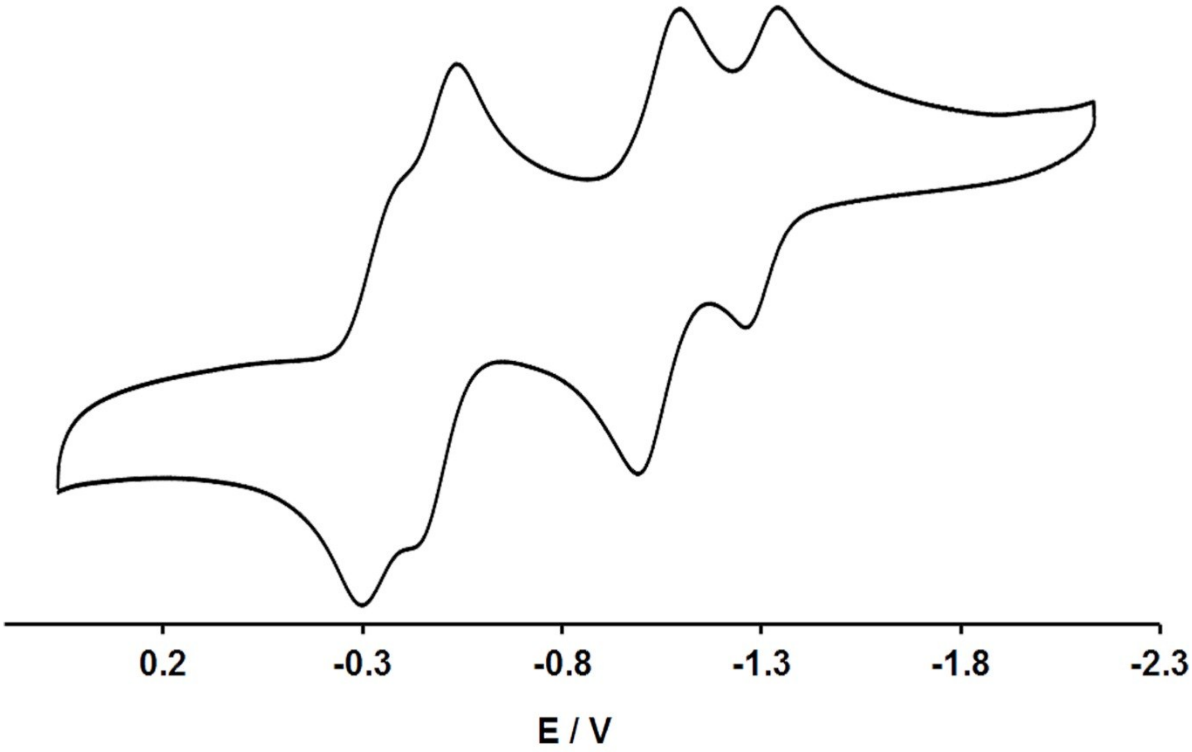

Figure S5: Cyclic voltammogram of dication **4** recorded in dichloromethane (nBu$_4$NPF$_6$ 0.1M, 100mVs^{-1} vs. Fc/Fc$^+$).

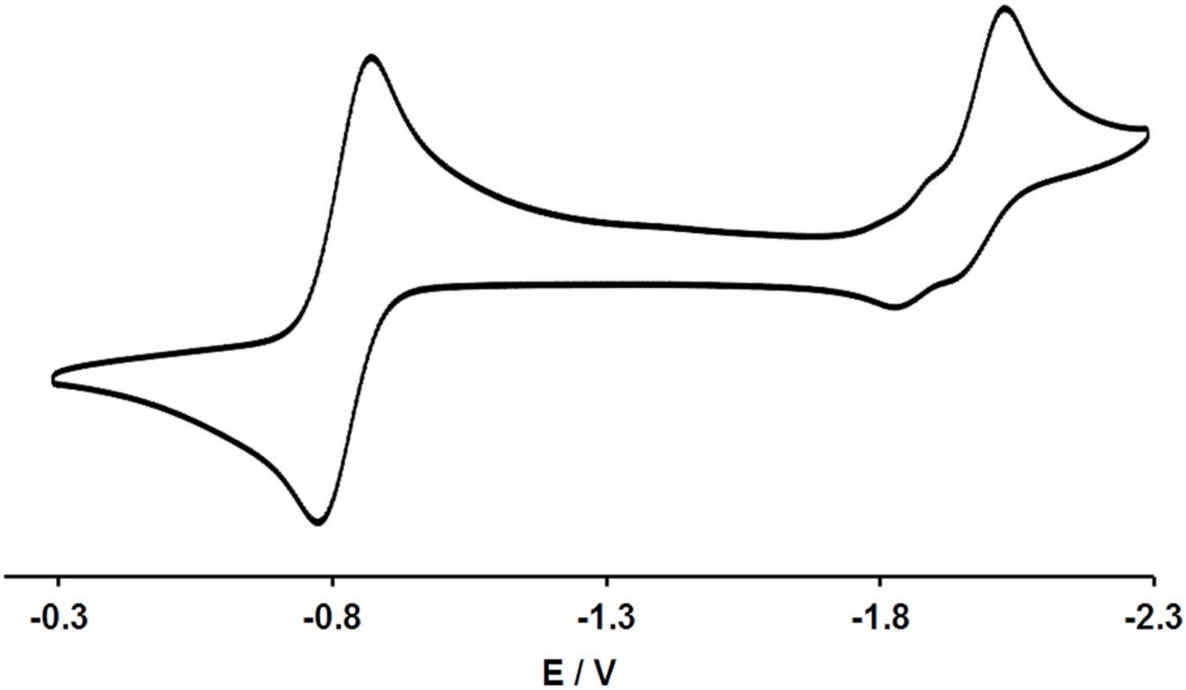

Figure S6: Cyclic voltammogram of iminium ion **S1** recorded in dichloromethane (nBu$_4$NPF$_6$ 0.1M, 100mVs^{-1} vs. Fc/Fc$^+$).

EPR SPECTROSCOPY

General Considerations: All EPR spectra were recorded on an X-band Active Spectrum Benchtop Micro ESR spectrometer (9.5 GHz, 300 Gauss sweep range). Field calibration was accomplished by using a standard of solid 2,2-diphenyl-1-picrylhydrazyl (DPPH), *g* = 2.0036. Spectra were recorded at room temperature in either benzene (**3a-c**) or dichloromethane (**5**).

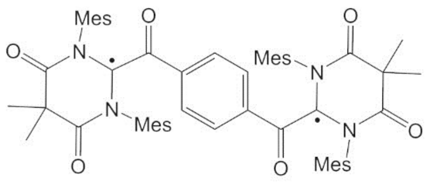

5

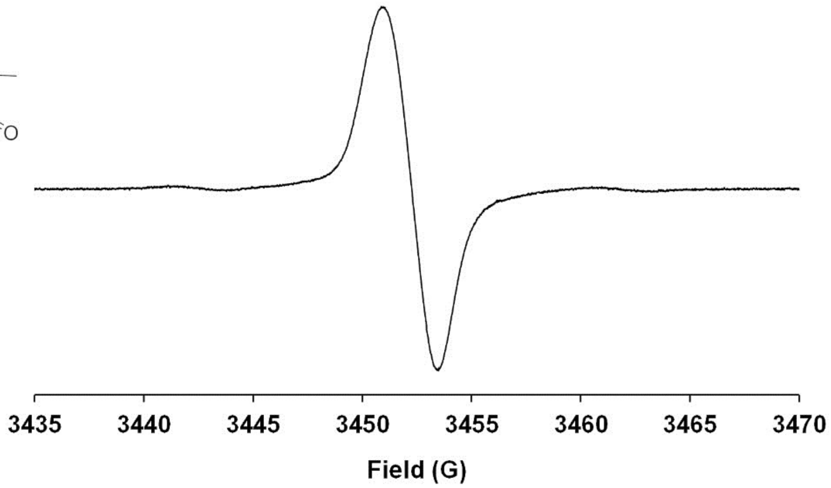

Figure S7: EPR spectrum of radical **5** recorded in solution in dichloromethane at room temperature.

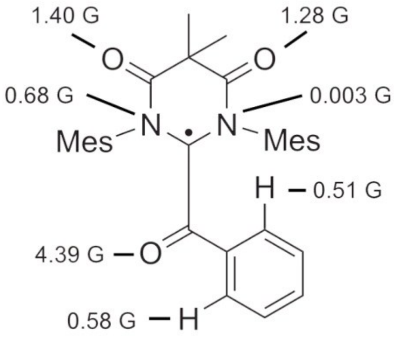

3a

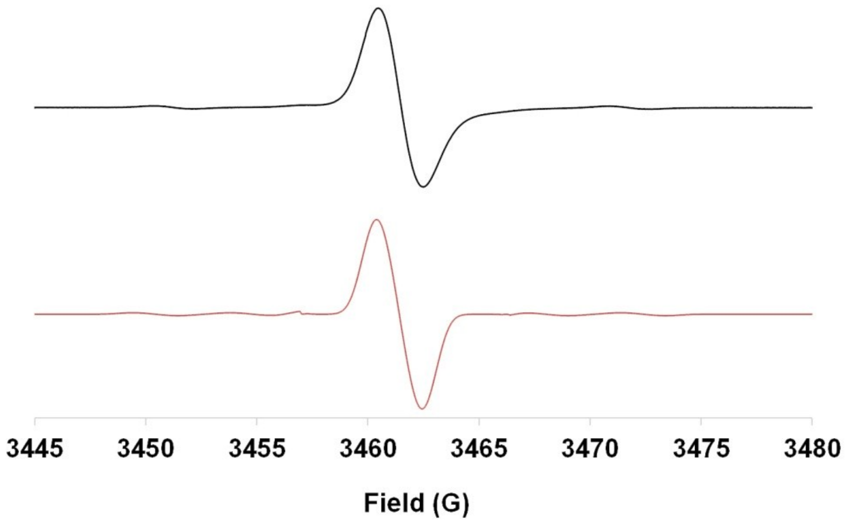

Figure S8: EPR spectra (experimental top right, simulated bottom right) of radical **3a** recorded in solution in benzene at room temperature. Hyperfine coupling constants are provided (left).

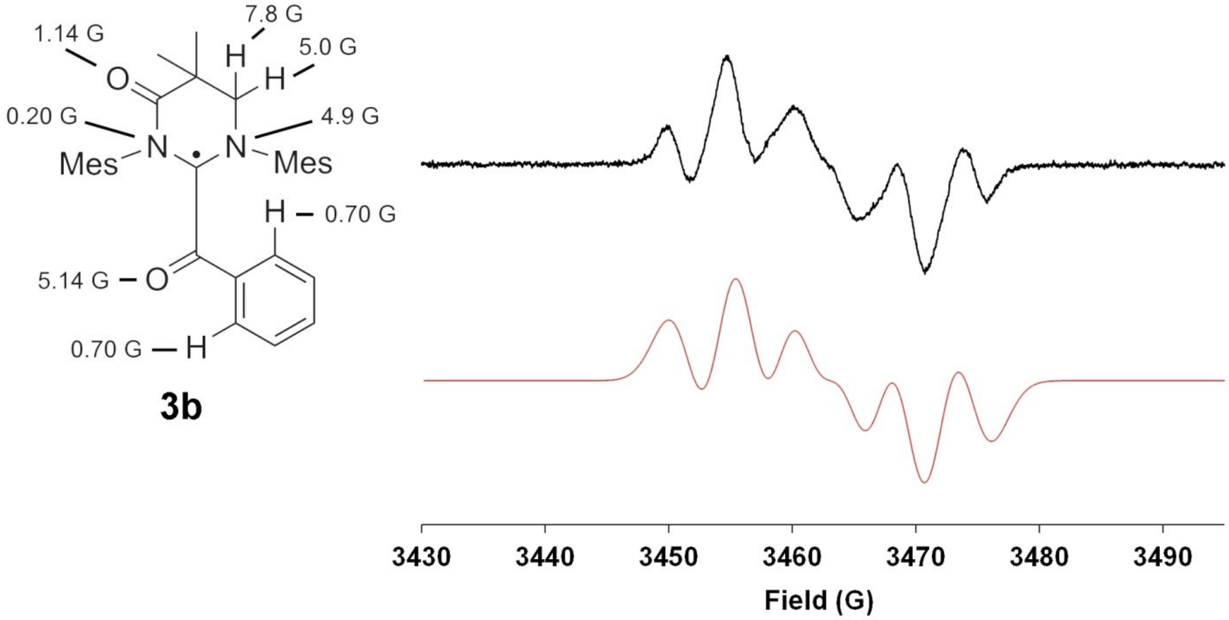

Figure S9: EPR spectra (experimental top right, simulated bottom right) of radical **3b** recorded in solution in benzene at room temperature. Hyperfine coupling constants are provided (left).

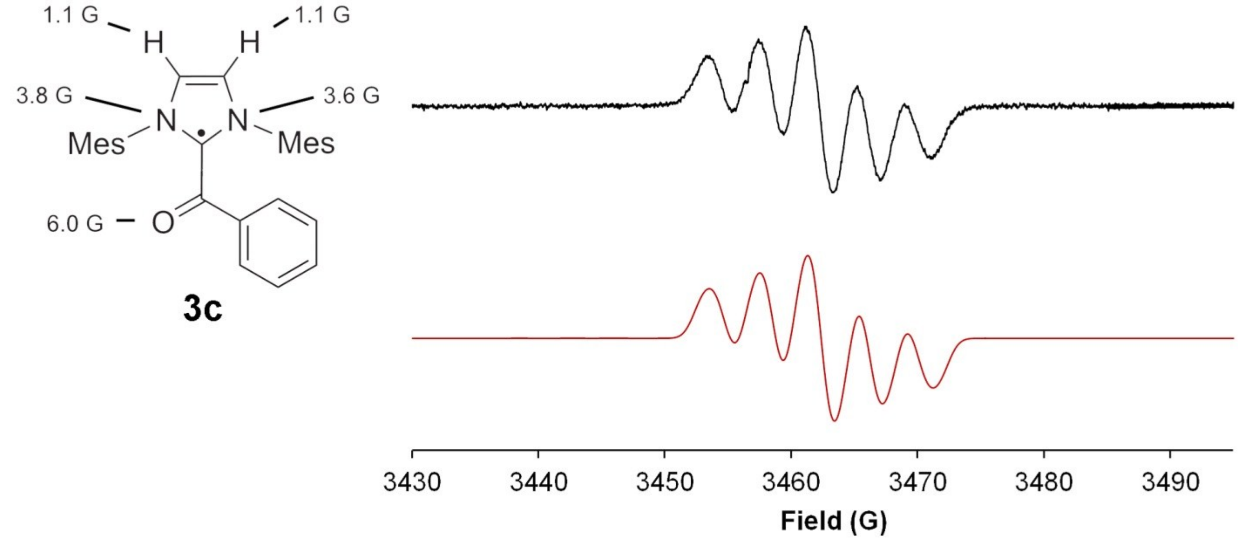

Figure S10: EPR spectra (experimental top right, simulated bottom right) of radical **3c** recorded in solution in benzene at room temperature. Hyperfine coupling constants are provided (left).

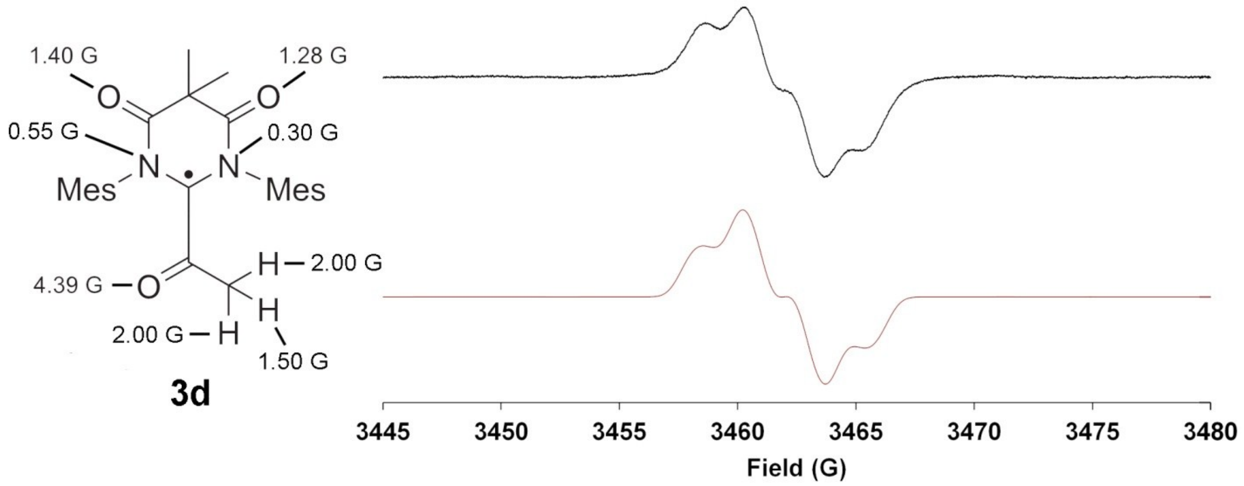

Figure S11: EPR spectra (experimental top right, simulated bottom right) of radical **3d** recorded in solution in benzene at room temperature. Hyperfine coupling constants are provided (left).

Discussion of EPR Data:

The degree of hyperfine coupling to the ^{14}N nuclei of the carbene ligand is dependent on the number of carbonyl groups present. The EPR spectra for radicals **3a** and **3d** are essentially identical with the exception that **3a** exhibits minor through-space coupling to the two *o*-hydrogens on the phenyl substituent whereas **3d** exhibits coupling to the three methyl hydrogens. Surprisingly, no significant coupling to the nitrogen atoms of the diamidocarbene was observed. In contrast, the EPR spectrum of **3b** was more complex with hyperfine coupling to the nitrogen nucleus of the amino functionality ($a(^{14}N) = 4.9$ G) as well as the CH_2 group in the MAAC backbone ($a(^{1}H) = 7.8$ and 5.0G). For radical **3c**, which does not contain a carbonyl group, hyperfine coupling to both nitrogen atoms was observed ($a(^{14}N_A) = 3.8$ G, $a(^{14}N_B) = 3.6$ G). Interestingly, the localization of the spin density (see Figure 4 in the text) on the C1 carbon was found to decrease from approximately 50–20% as the number of carbonyl groups decreased (53.0%, 51.8%, 42.5%, and 20.9% for **3d**, **3a**, **3b**, and **3c**; respectively). The spin density on the C2 carbon was found to increase (0.4%, 1.3%, 6.0%, 14.4% for **3d**, **3a**, **3b**, and **3c**, respectively) concomitant with increased 1-electron π bonding between the carbene and acyl centres.

These observations are both consistent with the CV data, and reflect the decrease in π acidity of the carbene ligand when going from the DAC to the MAAC to the NHC. In all cases, the second primary spin carrier was the O3 atom of the acyl fragment with densities ranging from 19.3–29.6%. In agreement with the experimental data, there is negligible spin density on N1 and N2 in the DAC in radicals **3a** and **3d** (1.7% and 3.5%, respectively), whereas a greater degree spin density is localized on the amino nitrogen 1in **3b** with minimal contribution from the amido nitrogen (12.0% for N1, 1.5% for N2). In the NHC-derived radical **3c**, there was near equal localization of the spin density on both nitrogen atoms (~12%).

CRYSTALLOGRAPHY

General Considerations: All crystallographic measurements were carried out on a Rigaku Mini CCD area detector diffractometer using graphite-monochromated Mo Kα radiation (λ = 0.71073 Å) at 223 K using an Oxford Cryostream low-temperature device. A sample of suitable size and quality was selected and mounted onto a nylon loop. Data reductions were performed using Crystal Clear Expert 2.0. The structures were solved by direct methods, which successfully located most of the non-hydrogen atoms. Subsequent refinements on F^2 using the SHELXTL/PC package (version 5.1) allowed location of the remaining non-hydrogen. Colorless, single crystals of **2a** were obtained by slow diffusion of hexanes into a dichloromethane saturated with the compound. **2a** crystallized in the monoclinic space group $P2_1/c$ with one interstitial molecule of HCl in the asymmetric unit (presumably formed from the presence of water in the crystallization solvent). Colorless crystals of **2b** and **2c** were grown by slow diffusion of hexanes into a dichloromethane solutions saturated with each compound at -35°C for several days. These two compounds the monoclinic space group $P2_1/c$ and the triclinic space group *P–1*, respectively. Red single crystals of **3a** were obtained by cooling a hexanes solution saturated with the compound to -35°C for several days. This compound crystallized in the monoclinic space group $P2_1/c$. Key details of the crystal and structure refinement data are summarized in Table S1. Further crystallographic details may be found in the respective CIF files which were deposited at the Cambridge Crystallographic Data Centre, Cambridge, UK. The CCDC reference numbers for **2a**, **2b**, **2c**, and **3a** were assigned as 1025142, 1025143, 1025144, and 1025145, respectively.

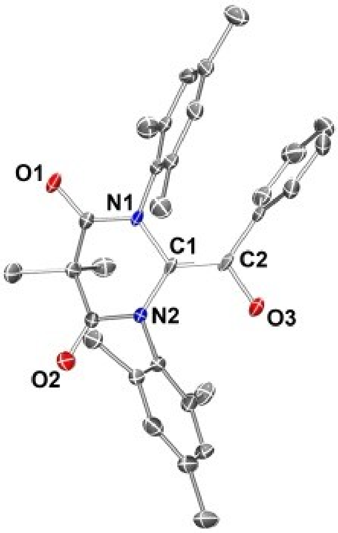

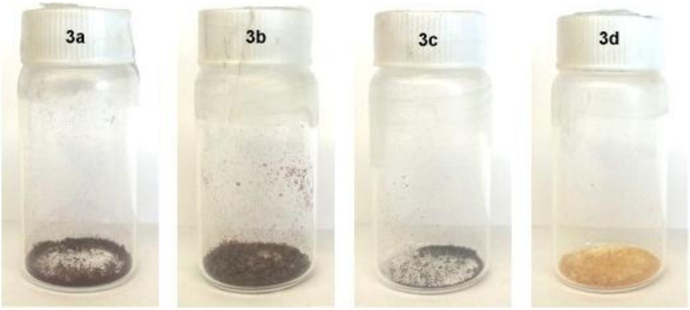

Figure S12: (left): ORTEP diagrams of **3a**; the thermal ellipsoids are drawn at 50% probability and H-atoms have been omitted for clarity. (right): solid powders of **3a–d** indicating color.

Table S2. Crystal Data, Data Collection and Structure Refinement for **2a**–HCl, **2b**, **2c**–CH_2Cl_2, and **3a**

	2a –HCl	**2b**	**2c** – CH_2Cl_2	**3a**
Empirical Formula	$C_{31}H_{34}N_2O_3Cl_2$	$C_{31}H_{35}N_2O_2Cl$	$C_{35}H_{43}Cl_3N_2O$	$C_{31}H_{33}N_2O_3$
Formula Weight	553.50	503.06	614.06	481.59
Temperature	100(2) K	223(2) K	223(2) K	223(2) K
Wavelength	0.71075 Å	0.71075 Å	0.71075 Å	0.71075 Å
Crystal System	Monoclinic	Monoclinic	Triclinic	Monoclinic
Space Group	P2(1)/c	P2(1)/c	*P–1*	P2(1)/c
Unit Cell Dimensions	a = 9.4917(7) Å	a = 10.4748(10) Å	a = 11.4742(18)Å	a = 11.8892(10)Å
	b = 18.4515(14) Å	b = 17.8218(17)Å	b = 11.8275(19) Å	b = 16.2557(14) Å
	c = 16.3576(12) Å	c = 15.4388(14) Å	c = 12.891(2) Å	c = 13.7767(12) Å
	α= 90°	α= 90°	α= 81.869(6)°	α= 90°
	β= 100.110(2)°	β= 105.179(7)°	β= 87.309(6)°	β= 96.327(7)°
	γ = 90°	γ = 90°	γ = 88.774(6)°	γ = 90°
Volume	2820.3(4) Å^3	2781.6(5) Å^3	1729.8(5) Å^3	2646.4(4) Å^3
Z	4	4	2	4
Density (calculated)	1.304 Mg/m3	1.201 Mg/m3	1.179 Mg/m^3	1.209 Mg/m^3
Absorption coefficient	0.265 mm^{-1}	0.167 mm^{-1}	0.293 mm^{-1}	0.078 mm^{-1}
F(000)	1168	1072	652	1028
Crystal size	0.40 x 0.16 x 0.09 mm^3	0.48 x 0.12 x 0.12 mm^3	0.11 x 0.07 x 0.06 mm^3	0.21 x 0.18 x 0.17 mm^3
Theta range for data collections	3.04 to 25.00°	3.05 to 24.00°	3.06 to 24.00°	3.04 to 25.00°
Index ranges	-11<=h<=11, -21<=k<=21, -19<=l<=19	-11<=h<=11, -20<=k<=20, -17<=l<=17	-13<=h<=13, -13<=k<=13, -14<=l<=14	-14<=h<=14, -19<=k<=19, -16<=l<=16
Reflections collected	52026	21407	13521	22167
Independent reflections	4961 [R(int) = 0.0387]	4354 [R(int) = 0.0983]	5427 [R(int) = 0.1337]	4656 [R(int) = 0.0520]
Completeness to theta = 26.00°	99.8 %	99.8 %	99.8 %	99.8 %
Refinement method	Full-matrix least-squares on F^2	Full-matrix least-squares on F^2	Full-matrix least-squares on F^2	Full-matrix least-squares on F^2
Data/restraints/parameters	4961 / 0 / 355	4354 / 0 / 333	5427 / 33 / 378	4656 / 0 / 333
GooF on F^2	1.011	1.008	1.004	1.004
Final R indices [I>2sigma(I)]	R1 = 0.0355, wR2 = 0.0844	R1 = 0.0570, wR2 = 0.0931	R1 = 0.0786, wR2 = 0.1302	R1 = 0.0508, wR2 = 0.0875
R indices (all data)	R1 = 0.0392, wR2 = 0.0868	R1 = 0.1093, wR2 = 0.1093	R1 = 0.1924, wR2 = 0.1685	R1 = 0.0788, wR2 = 0.0984
Largest diff. peak and hole	0.713 and -0.343 e.Å^{-3}	0.204 and -0.229 e.Å^{-3}	0.272 and -0.250 e.Å^{-3}	0.422 and -0.148 e.Å^{-3}

COMPUTATIONAL DATA

General Considerations:

We performed full geometry optimization calculations of all compounds with Gaussian09[3] using the Becke exchange functional and the Lee-Yang-Parr correlation functional (B3LYP)[4], [5] and using the 6-311G**[6,7] basis set for all atoms. Frequency calculations were also performed at the same level of theory. It was determined that the geometries were at their minima due to the lack of imaginary frequencies. The computed structures were compared to the respective X-ray structures when available to ensure that the experimental and calculated data were in good agreement. The optimized geometries from the DFT analyses were used as input geometries for EPR analyses for all compounds.

Wireframe rendering and Cartesian coordinates for 3a:

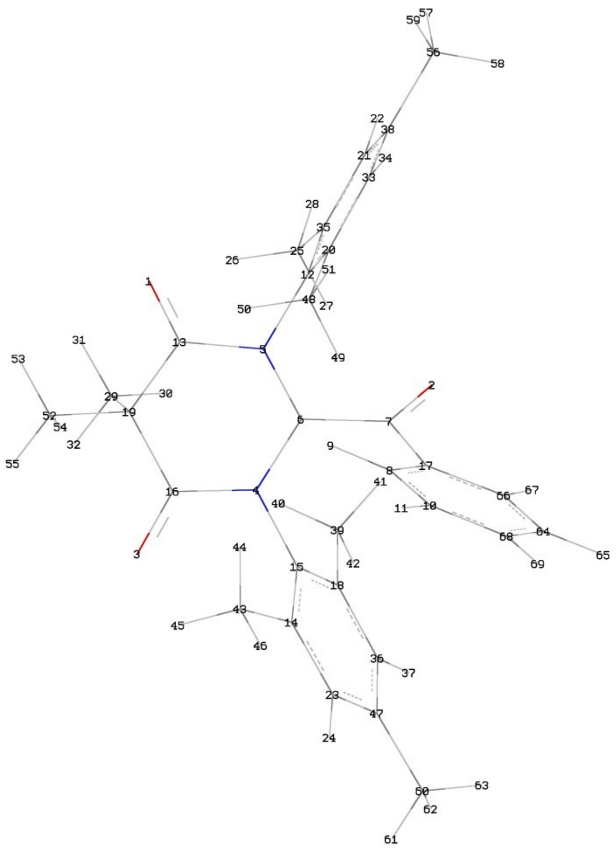

Center	Coordinates			Center	Coordinates		
Number	X	Y	Z	Number	X	Y	Z
1	2.93805	2.547232	-0.25806	36	-3.53332	0.027188	2.256295
2	0.693026	-1.74909	1.123609	37	-3.64939	-0.18266	3.314978
3	-1.62455	3.264349	-0.23054	38	5.000104	-1.63779	0.524027
4	-0.84166	1.128868	-0.09004	39	-1.15646	0.629683	2.779281
5	1.530572	0.773025	-0.00181	40	-0.58618	1.53833	2.573028
6	0.238424	0.241887	-0.02641	41	-0.45904	-0.21204	2.760928
7	0.020453	-1.18664	0.255193	42	-1.55466	0.710498	3.791913

8	-1.23978	-1.73244	-1.88022
9	-0.7575	-0.89984	-2.37778
10	-2.08607	-2.5696	-2.60262
11	-2.26621	-2.37792	-3.65442
12	2.705249	-0.08048	0.185723
13	1.810636	2.106245	-0.33646
14	-3.24251	0.659529	-0.4481
15	-2.14286	0.713389	0.422388
16	-0.69681	2.495505	-0.37059
17	-0.98324	-1.9752	-0.52718
18	-2.28449	0.446491	1.79401
19	0.660904	2.944427	-0.89329
20	3.318665	-0.12706	1.443388
21	4.377387	-1.54159	-0.71755
22	4.792492	-2.07809	-1.56498
23	-4.46676	0.233522	0.066406
24	-5.31819	0.176587	-0.60465
25	2.630904	-0.66134	-2.29326
26	2.583348	0.376547	-2.63383
27	1.618504	-1.07193	-2.32739
28	3.234058	-1.21717	-3.01254
29	0.657656	2.77516	-2.43941
30	0.497848	1.738165	-2.74215
31	1.615694	3.109388	-2.84222
32	-0.13776	3.387705	-2.86844
33	4.459881	-0.91255	1.587331
34	4.940486	-0.95659	2.559789
35	3.235232	-0.76099	-0.91456
43	-3.16631	1.109199	-1.884
44	-2.21185	0.861203	-2.34796
45	-3.28195	2.195865	-1.93533
46	-3.96003	0.64948	-2.4751
47	-4.6317	-0.10586	1.408757
48	2.77656	0.645606	2.615295
49	1.765351	0.315955	2.861287
50	2.745317	1.716905	2.40017
51	3.403896	0.49744	3.495618
52	0.88532	4.423001	-0.53944
53	1.85034	4.747654	-0.92584
54	0.882934	4.572469	0.542169
55	0.087136	5.029043	-0.96589
56	6.215865	-2.51001	0.721945
57	6.708657	-2.72906	-0.22766
58	5.940171	-3.46634	1.17945
59	6.94572	-2.03263	1.380824
60	-5.95912	-0.60283	1.926101
61	-6.79373	-0.13106	1.402118
62	-6.07129	-0.40298	2.993964
63	-6.05251	-1.68489	1.78255
64	-2.43401	-3.91134	-0.62803
65	-2.89816	-4.76042	-0.13899
66	-1.57696	-3.08525	0.087595
67	-1.34726	-3.28624	1.12639
68	-2.69096	-3.65635	-1.97603
69	-3.35203	-4.30779	-2.53657

Wireframe rendering and Cartesian coordinates for 3b:

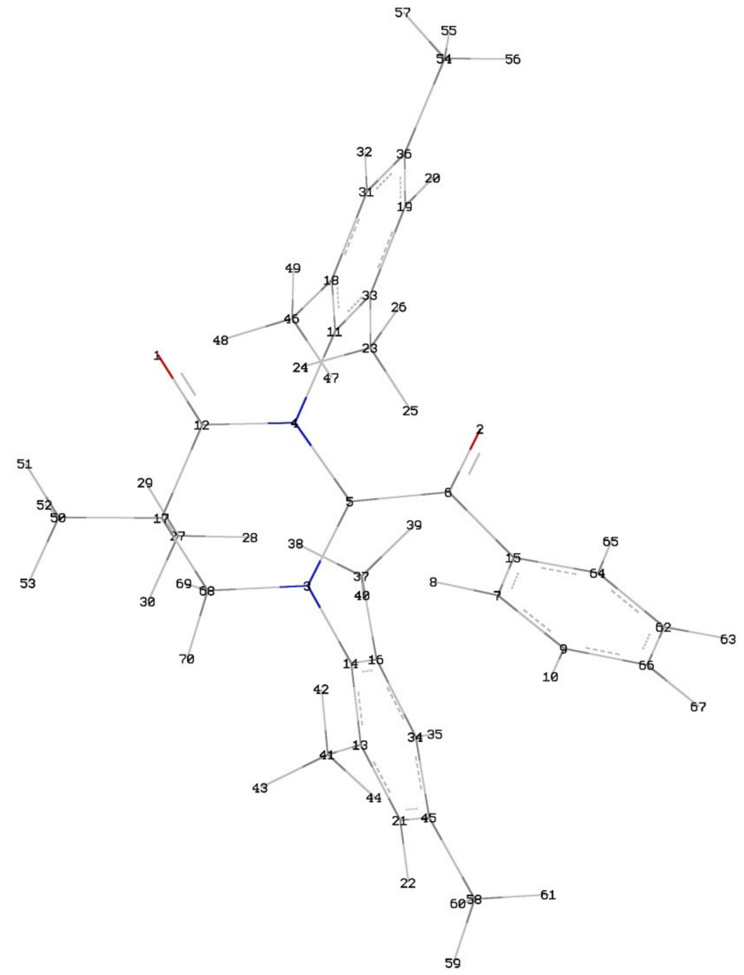

Center		Coordinates		Center		Coordinates	
Number	X	Y	Z	Number	X	Y	Z
1	2.944925	2.55387	-0.37739	36	4.998319	-1.55992	0.518095
2	0.747659	-1.76221	1.014806	37	-1.1976	0.489663	2.746148
3	-0.86582	1.141042	-0.1346	38	-0.50747	1.31749	2.57228
4	1.506704	0.823251	0.008781	39	-0.61218	-0.43197	2.697927
5	0.206252	0.275242	-0.01304	40	-1.58488	0.588962	3.761803
6	0.0165	-1.15354	0.212798	42	-2.16421	1.14964	-2.29933
7	-1.40067	-1.64106	-1.84585	43	-3.42908	2.346477	-2.02476
8	-0.95454	-0.796	-2.35565	44	-3.86162	0.716877	-2.53397
9	-2.29707	-2.4601	-2.52723	45	-4.73879	0.20363	1.378909
10	-2.55012	-2.24185	-3.55903	46	2.740101	0.67613	2.622899

11	2.684117	-0.02785	0.190275	47	1.741404	0.308806	2.869084
12	1.803654	2.137443	-0.38683	48	2.669402	1.747152	2.414425
13	-3.28295	0.860102	-0.46644	49	3.375219	0.545749	3.50067
14	-2.17062	0.787237	0.389979	50	0.934736	4.467502	-0.65486
15	-1.04507	-1.91605	-0.52075	51	1.86409	4.751315	-1.14721
16	-2.3394	0.484684	1.757519	52	1.046307	4.680736	0.411155
17	0.637053	2.981178	-0.90049	53	0.122012	5.085133	-1.04808
18	3.301	-0.07416	1.445216	54	6.224741	-2.41893	0.709877
19	4.369585	-1.46852	-0.72088	55	6.719262	-2.62645	-0.24156
20	4.786502	-2.00081	-1.57028	56	5.961631	-3.38151	1.161895
21	-4.54597	0.557552	0.046532	57	6.949975	-1.93676	1.370609
22	-5.40045	0.597955	-0.62248	58	-6.10585	-0.16601	1.9
23	2.600776	-0.6101	-2.2856	59	-6.89811	0.306299	1.314923
24	2.574129	0.423421	-2.64246	60	-6.22946	0.132899	2.943716
25	1.578043	-0.99593	-2.29945	61	-6.26192	-1.24917	1.849872
26	3.18207	-1.19194	-3.00258	62	-2.49827	-3.85662	-0.57293
27	0.493103	2.723547	-2.41707	63	-2.92187	-4.72182	-0.07482
28	0.273413	1.677802	-2.63791	64	-1.59197	-3.04691	0.100666
29	1.416369	2.995076	-2.93287	65	-1.28115	-3.28016	1.111309
30	-0.31777	3.335295	-2.82241	66	-2.85557	-3.56597	-1.88999
31	4.451921	-0.84555	1.585528	67	-3.55444	-4.20414	-2.41923
32	4.933825	-0.88942	2.557567	68	-0.62897	2.58878	-0.14468
33	3.217732	-0.70118	-0.91212	69	-0.5632	2.953385	0.890365
34	-3.62284	0.189203	2.216671	70	-1.49949	3.070677	-0.59509
35	-3.75342	-0.04558	3.268763				

Wireframe rendering and Cartesian coordinates for 3c:

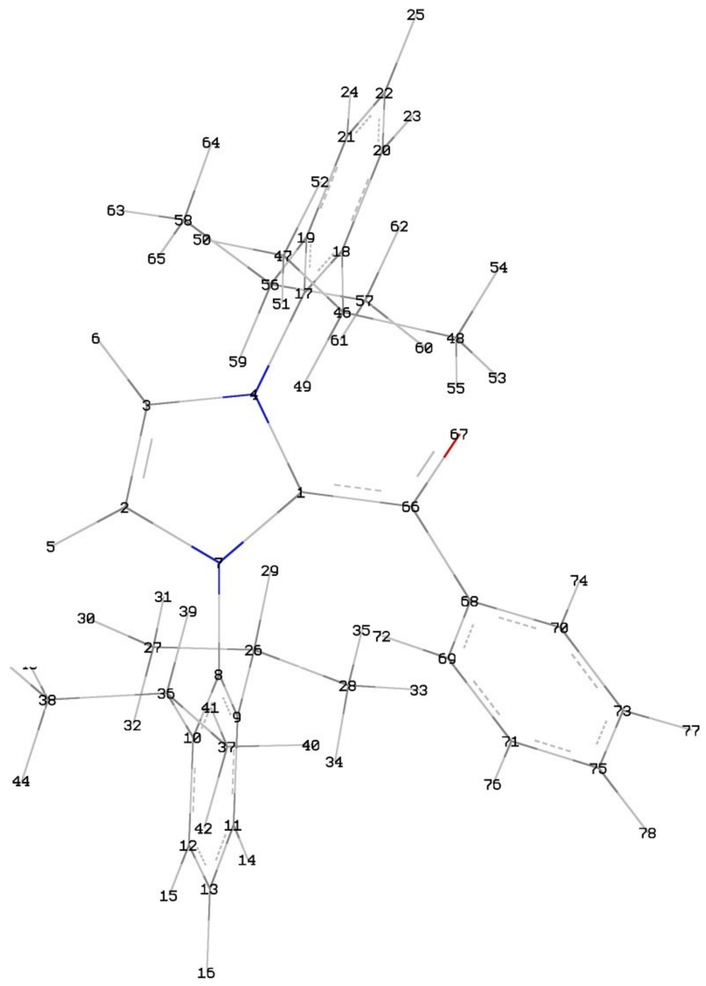

Center		Coordinates		Center		Coordinates	
Number	X	Y	Z	Number	X	Y	Z
1	0.275711	0.011133	-0.13394	40	-3.37286	3.042705	-0.11793
2	-0.12653	-0.07602	-2.37042	41	-3.14759	4.023312	-1.57156
3	1.207416	0.001493	-2.20449	42	-4.57829	3.008732	-1.40548
4	1.474827	0.043451	-0.8438	43	-2.4238	1.198813	-3.94614
5	-0.7155	-0.16557	-3.26485	44	-4.03894	1.836039	-3.64526
6	2.002074	0.036679	-2.92888	45	-2.67005	2.944069	-3.81191
7	-0.72664	-0.06936	-1.10858	46	2.281381	2.773114	-0.1359
8	-2.12011	-0.41047	-0.94849	47	2.790624	3.864566	-1.09446
9	-2.47225	-1.70226	-0.50705	48	2.016303	3.3418	1.271777
10	-3.09354	0.536455	-1.33334	49	1.324994	2.422564	-0.52851

11	-3.8325	-2.00545	-0.40656	50	2.952769	3.467832	-2.10032
12	-4.43767	0.169278	-1.22941	51	2.062282	4.678041	-1.16388
13	-4.80788	-1.08241	-0.7584	52	3.734173	4.296886	-0.75001
14	-4.13122	-2.98899	-0.06469	53	1.659753	2.562337	1.947506
15	-5.20597	0.877012	-1.51739	54	2.927909	3.768035	1.70117
16	-5.85712	-1.34316	-0.67581	55	1.263831	4.135061	1.229521
17	2.812309	0.265913	-0.34149	56	3.218989	-2.26672	-0.46221
18	3.226582	1.579913	-0.06497	57	3.234578	-3.05638	0.860717
19	3.681608	-0.8336	-0.23404	58	4.036393	-2.97739	-1.55567
20	4.555334	1.773214	0.324637	59	2.182607	-2.23263	-0.80276
21	5.000827	-0.58348	0.148957	60	2.634596	-2.54009	1.611483
22	5.437305	0.706126	0.425481	61	2.828481	-4.06154	0.708068
23	4.902305	2.774356	0.553346	62	4.253535	-3.16408	1.244896
24	5.692282	-1.41262	0.246684	63	4.00565	-2.42848	-2.50117
25	6.464731	0.87827	0.726982	64	5.086232	-3.08539	-1.26879
26	-1.44426	-2.79507	-0.22818	65	3.639385	-3.98103	-1.73453
27	-1.40286	-3.79777	-1.39965	66	0.239661	-0.07759	1.299083
28	-1.68762	-3.52014	1.106616	67	1.287285	-0.46154	1.891544
29	-0.45952	-2.33357	-0.16015	68	-0.95267	0.292734	2.108681
30	-1.17557	-3.29913	-2.34547	69	-1.85503	1.303961	1.755409
31	-0.63462	-4.55652	-1.22377	70	-1.10011	-0.31941	3.365184
32	-2.36252	-4.31057	-1.51359	71	-2.89209	1.667414	2.609885
33	-1.75005	-2.81297	1.935358	72	-1.72024	1.836562	0.823277
34	-2.60956	-4.10854	1.089334	73	-2.1402	0.036826	4.214136
35	-0.86395	-4.20992	1.309482	74	-0.3684	-1.06164	3.658724
36	-2.73924	1.914367	-1.89011	75	-3.04647	1.029974	3.839115
37	-3.50558	3.058786	-1.20062	76	-3.57413	2.460713	2.323087
38	-2.97895	1.973525	-3.41295	77	-2.24171	-0.45413	5.176146
39	-1.67419	2.083672	-1.71639	78	-3.85417	1.313968	4.504431

Wireframe rendering and Cartesian coordinates for 3d:

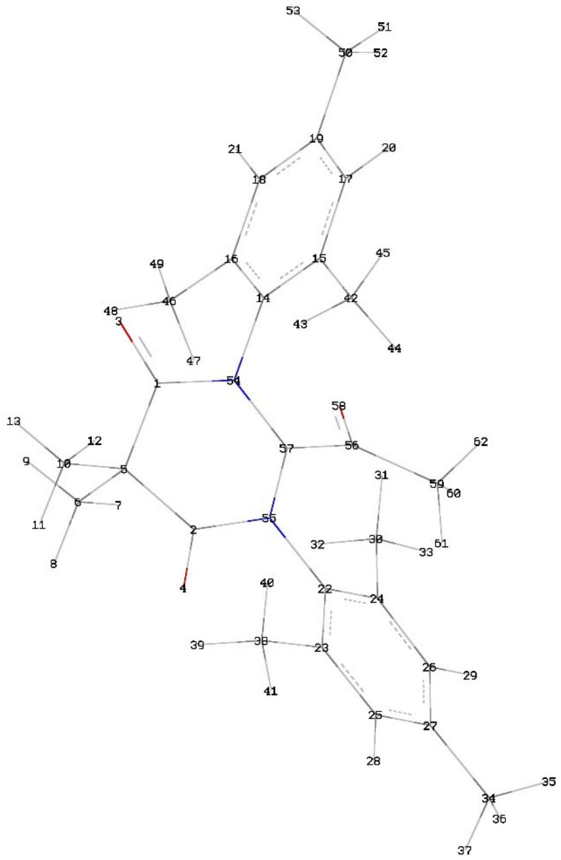

Center		Coordinates		Center		Coordinates	
Number	X	Y	Z	Number	X	Y	Z
1	0.13584	-0.13245	-0.00433	32	0.00680	0.01352	0.00263
2	-0.17195	0.03828	0.00498	33	-0.00770	-0.00159	0.01194
3	-0.12115	0.00855	0.00196	34	0.03320	0.00511	-0.00184
4	0.08377	-0.09601	-0.00178	35	-0.00596	-0.01254	0.00745
5	-0.00205	0.03730	-0.00013	36	-0.00945	0.01040	0.00715
6	-0.00060	0.00511	0.00084	37	-0.00735	-0.00132	-0.01220
7	-0.00317	-0.00575	-0.01392	38	-0.01708	-0.00327	0.02630
8	-0.00797	0.01114	-0.00033	39	0.00695	0.01356	-0.00245
9	0.01292	-0.00028	0.00030	40	0.01117	-0.00956	-0.00175
10	-0.00112	0.00552	-0.00119	41	-0.00778	-0.00155	-0.01168
11	-0.00793	0.01117	0.00047	42	0.01147	-0.01371	-0.02661
12	-0.00319	-0.00572	0.01411	43	0.00377	0.01466	0.00285
13	0.01286	-0.00034	-0.00032	44	-0.01161	0.00126	0.00398

14	-0.02761	0.01101	-0.00109	45	0.00425	-0.00637	0.01193
15	-0.01225	0.01244	0.02476	46	0.01025	-0.01386	0.02624
16	-0.01286	0.01267	-0.02695	47	-0.01440	0.00027	-0.00136
17	-0.00021	0.00029	-0.00282	48	0.00432	0.01474	-0.00265
18	-0.00013	0.00068	0.00369	49	0.00485	-0.00641	-0.01174
19	0.01515	-0.01487	-0.00006	50	-0.02086	0.02645	-0.00005
20	-0.00369	0.00468	-0.00822	51	0.00965	-0.00169	0.01118
21	-0.00383	0.00475	0.00837	52	-0.00547	-0.01544	0.00022
22	0.02877	0.00996	-0.00137	53	0.00927	-0.00192	-0.01127
23	0.01881	0.00355	-0.02710	54	0.01282	0.09866	-0.00830
24	0.01490	0.00352	0.02670	55	0.07810	0.01737	0.01164
25	-0.00042	-0.00025	0.00429	56	-0.32728	-0.69067	-0.01029
26	0.00126	-0.00032	-0.00150	57	0.31344	0.68933	0.00063
27	-0.02118	-0.00312	-0.00261	58	0.00557	-0.02718	0.00223
28	0.00612	0.00088	0.00854	59	-0.00911	-0.00196	-0.01134
29	0.00581	0.00095	-0.00816	60	0.00429	0.00005	0.00919
30	-0.01804	0.00007	-0.02517	61	-0.01507	-0.00549	0.00195
31	0.00499	-0.00058	0.00577	62	0.00712	-0.01366	-0.00169

REFERENCES

1 T. W. Hudnall, J. P. Moerdyk and C. W. Bielawski, *Chem. Commun.* 2010, **46**, 4288-4290.

2 J. K. Mahoney, D. Martin, C. E. Moore, A. L. Rheingold and G. Bertrand, *J. Am. Chem. Soc.* 2013, **135**, 18766-18769.

3 M. J. Frisch, G. W. Trucks, H. B. Schlegel, G. E. Scuseria, M. A. Robb, J. R. Cheeseman, G. Scalmani, V. Barone, B. Mennucci, G. A. Petersson, H. Nakatsuji, M. Caricato, X. Li, H. P. Hratchian, A. F. Izmaylov, J. Bloino, G. Zheng, J. L. Sonnenberg, M. Hada, M. Ehara, K. Toyota, R. Fukuda, J. Hasegawa, M. Ishida, T. Nakajima, Y. Honda, O. Kitao, H. Nakai, T. Vreven, J. Montgomery, J. A. , J. E. Perelta, F. Ogliaro, M. Bearpark, J. J. Heyd, E. Brothers, K. N. Kudin, V. N. Staroverov, T. Keith, R. Kobayashi, J. Normand, K. Raghavachari, A. Rendell, J. C. Burant, S. S. Iyengar, J. Tomasi, M. Cossi, N. Rega, J. M. Millam, M. Klene, J. E. Knox, J. B. Cross, V. Bakken, C. Adamo, J. Jaramillo, R. Gomperts, R. E. Stratmann, O. Yazyev, A. J. Austin, R. Cammi, C. Pomelli, J. W. Ochterski, R. L. Martin, K. Morokuma, V. G. Zakrzewski, G. A. Voth, P. Salvador, J. J. Dannenberg, S. Dapprich, A. D. Daniels, O. Farkas, J. B. Foresman, J. V. Ortiz, J. Cioslowski and D. J. Fox, *GAUSSIAN 09 (Revision C.01)*, (2010) Gaussian, Inc, Wallingford, CT.

4 C. Lee, W. Yang and R. G. Parr, *Phys. Rev. B: Condens. Matter* 1988, **37**, 785-789.

5 A. D. Becke, *J. Chem. Phys.* 1993, **98**, 5648-5652.

6 A. D. McLean and G. S. Chandler, *J. Chem. Phys.* 1980, **72**, 5639-5648.

7 T. Clark, J. Chandrasekhar, G. W. Spitznagel and P. v. R. Schleyer, *J. Comput. Chem.* 1983, **4**, 294-301.